性物質と定義することができる．*In vitro* 遺伝毒性試験は陽性反応を示しやすく，その毒性メカニズムが不明であることもある．強い細胞毒性，高浸透圧，沈殿の生成，非生理的 pH などは非特異的な影響により陽性反応を示すこともあるので注意を要する．通常，1つの遺伝毒性試験の結果から遺伝毒性の有無を判定することは困難であり，複数の試験結果から試験条件や反応の程度などを考慮して判定することが多い．遺伝毒性試験で陰性を示すもの，また陽性を示しても非 DNA 損傷性であるものを総称して非遺伝毒性物質と呼ぶこともある．

4 遺伝毒性物質に閾値はあるのか？

遺伝毒性物質が DNA と反応し遺伝子突然変異をもたらす．突然変異は確率論的(stochastic)事象であり 0 になることはない．また，たった1つの遺伝子突然変異でも，その変異ががん遺伝子，がん抑制遺伝子などの細胞のがん化に重要な遺伝子に生じた場合，1つのがん原細胞が生じ，それだけで発がんに至ることがある．したがって，この発がんの確率も 0 にはならず，理論的に遺伝毒性発がん物質に閾値を設定することはできない．

一方，タンパク質に作用する非遺伝毒性発がん物質に関してはどうであろうか？ 1つの細胞中には遺伝子は多くても 2 コピーしか存在しないのに対して，タンパク質分子は数多く存在する．高濃度の化学物質が多くのタンパク質と作用すれば発がんに至る影響が表れるかもしれないが，少数であれば影響はないことは容易に想像できる．このようなことから非遺伝毒性発がん物質に関しては理論的に閾値が設定できる．また，幾つかの実験により非遺伝毒性発がん物質の閾値の存在は証明されており，多くの専門家はこの問題に関して異論はない．問題は遺伝毒性発がん物質の閾値である．

遺伝毒性発がん物質の発がん性，遺伝毒性，DNA 付加体の形成に閾値が存在するかどうかの検討が多くの研究者によって動物実験等によってなされている．アフラトキシン B1 やペンツピレンを動物に投与した場合，肝 DNA 付加体の形成は用量相関性を示す．DNA 付加体の検出は質量分析機の進歩により通常，人が曝露するレベルより 2 桁低いレベルの検出まで可能となっており，極低用量でも用量相関性が観察される．DNA 付加体の形成は化学反応であり，DNA と反応する化学物質が存在する限り形成を否定できないため閾値がないとするのが一般的である．

生物学的反応である遺伝毒性の閾値の存在の証明には，動物に投与する遺伝毒性物質の用量を段階的に下げて無作用量が存在するかどうかを，様々な遺伝毒性のエンドポイントで検出する方法がとられている．遺伝子突然変異試験の場合，無作用量とは自然誘発突然変異レベルを示す．このような実験は千～十万倍の用量域で行うため，用量を対数換算して表示することがしばしば見られる．図 2 は $y=ax+b$ の用量相関性を示す反応の 2 つのグラフを示す．これは閾値なしモデルであるが，対数表示だと閾値があるようにみえる．これは錯覚であり，このような図から閾値を論じるべきではない．同様に，低用量域ではその増加量が極くわずかで有意差がないため閾値とみなすとする論理もあるが，これも正しくない．それは試験の検出力が乏しく，自然突然変異の変動が大きいため統計的に有意にならないだけである．先に述べたように遺伝毒性は遺伝毒性試験によって認識される．すべての試験には検出限界があり，用量を段階的に下げて，無作用量が存在するかどうかをみるというストラテジーは，閾値よりもむしろ検出感度をみるに過ぎない．そもそも(閾値の)存在を，非検出をもって証明することが論理的に無理があるように思われる．

一方，極低用量域では高用量域からの一義的外挿では説明できない生物学的反応が効率的に働くため閾値を設定できるとの説もある．ここでの生物学的反応とは DNA 修復，代謝反応，

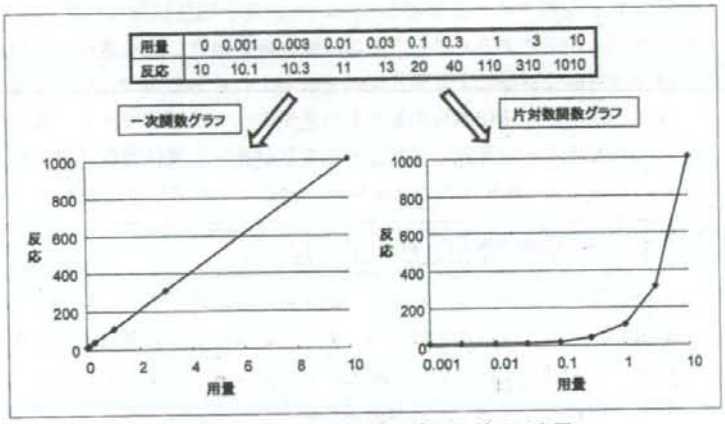

図2 閾値なし用量相関モデルのグラフ表示

スカベンジャーなどの防御機構が考えられる．しかしながら，このような防御機構は遺伝毒性の発生確率の低減化には寄与するが，閾値を作る根拠にはならない．DNA付加体の除去には塩基除去修復機構が働き，これは一般にエラー非発生型の修復機構であるが，10^{-5}以下の発生頻度でエラーが起き，突然変異を引き起こす．同様に，化学物質の無毒化に働く薬物代謝や，スカベンジャーも100%の効率で働くという保証はない．

このような科学的・理論的解釈では閾値を設定できないが，現実的には極低用量の遺伝毒性反応は，自然に起きる反応と区別をすることが困難であり，閾値と見なしてもいいのではないかという考え方もある．一般に遺伝子突然変異試験の自然突然変異頻度は10^{-6}程度であり，一定のばらつきを持つ．この原因として酸化ストレス，老化等の内的要因や，環境中に極微量存在する試験物質以外の化学物質や放射線，紫外線などの影響が考えられる．これにより，自然に起きる遺伝毒性反応内に収まるようなレベルを「現実的閾値(practical もしくは pragmatic threshold)」とするものである．しかし，これは閾値とは別の問題である．現実的閾値の考えはある種の妥協であり，専門家の中でもこの考えに合意はできていない．したがって，発がん物質が遺伝毒性試験陽性，特にそれが発がん標的組織であれば，その発がん性に閾値を設定することはできず，ADIのような安全量を設定することはできない．

5 遺伝毒性発がん物質のリスク管理

それでは，遺伝毒性発がん物質に閾値が設定できなければそのリスク管理はできないのであろうか？ 米国においては1958年に「発がん性の可能性がある化学物質はいかなる低用量でも安全とみなすことはできない」という，いわゆるデラニー条項により，動物に対して発がん性を示す農薬が残留する加工食品の販売が禁止され，その後，適用範囲が着色料，動物用薬品，飼料に拡大された．しかしながら，このゼロリスク思想は現実的には多くの矛盾点があった．主な矛盾点としては，①分析技術の進歩により，微量な化学物質も検出可能となり，検出限界である安全レベルがどんどん低くなってしまうこと．②発がん性の有無だけが強調されているため，他の毒性が低くて，安全性の高い化合物ができても，わずかの発がん性のため代替できないこと．③人工化学物質のみを対象としているため，天然由来の発がん物質は無視されていること．④動物実験の発がん性試験は，必ずしも人に対する発がん性と一致しないこと，などが挙げられる．

これらのことから，1996年「食品品質保護法」の制定とともにデラニー条項は廃止された．

閾値を設定しゼロリスクを追求するのに対して，「発がん可能性がある化学物質が十分に低濃度であれば，その発がん可能性は極めて小さくなり，その程度が社会的に許容できるリスクレベルであれば実質的に安全と見なし得る」とのリスク管理の方法もある．この量を実質安全性量(virtually safety dose；VSD)といい，そのリスクレベルを「無視しうる(negligible)」，もしくは「許容できる(acceptable)」リスクとする．ここでの許容できるリスクとしてのがんの生涯リスクレベルは一般的に百万分の1(10^{-6})が採用されている．10^{-6}の生涯リスクとは日本の人口(10^8)と，平均寿命(80)から計算すると($10^8 \times 1/80 \times 10^{-6} = 1.25$)1年間に1.25人のがんによる死者が増えることを意味する．がんは今や先進諸国では死亡原因の1位であり，我が国においても年間約35万人が，がんで死亡していることを考慮すると1.25人の増加は社会的に許容できるといえよう．VSDは一般にげっ歯類を用いた発がん試験で得られた半数がん誘発用量(TD 50)からマルチステージモデル，もしくは直線外挿により得られる(図3)．このような発がん化学物質を生涯発がんリスクレベルで評価し，管理に用いる手法は，現在，水道水や大気中に含まれる汚染物質の新しい環境基準値の設定に用いられている．

Cheesemanらは約500種類の発がん化学物質に関する動物実験でのTD 50からVSDを算出し，その算定曝露分布の結果から，ほとんどの発がん化学物質については0.5 μg/kg(0.5 ppb)以下の食事中濃度で百万分の1のがん生涯リスクよりも低くなることを示した．[1] 1人の1日食事量を3 kg(固形食品1.5 kg，飲料1.5 kg)とし，その化学物質が全食事にムラなく入っていると仮定すると，1日曝露量は1.5 μg/人と計算できる．つまり，大部分の化学物質については1日の摂取量が1.5 μg/人以下であれば，たとえそれが発がん物質であっても実質的な健康危害はほとんどないだろうとすることができる．このような包括的な閾値を「毒性学的懸念の閾値(threshold of toxicological concern；TTC)」という．TTCは化学構造を考慮すればその毒性が分かっていないものも含め，多くの化学物質に適用できる．我が国では食品衛生法に基づき残留農薬のポジティブリスト制が導入されたが，ここでは残留基準値が設定されていない農薬に関しては一律基準値として0.01 ppmが設定された．この値もTTC(1.5 μg/人)に基づくものであり，個々の農畜産物の1日摂取量は米を除いて150 gを超えることがないという国民栄養調査から計算されている(1.5/150＝0.01)．TTCは既に米国FDAがプラスチック容器から溶出する化学物質(間接添加物)のリスク管理に用いており，またJECFA(FAO/WHO合同食品添加物専門家委員会)は食品に添加する香料物質に適用している．

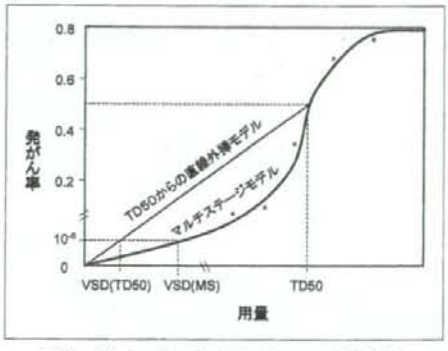

図3 Virtually Safety Doseの算出法

しかしながら，TTC レベルはその発がん物質に遺伝毒性があった場合にはより慎重な取り扱いが必要となる．Kroes らは 600 以上の発がん化学物質を比較して，TTC を 1.5 μg/人とした場合，遺伝毒性もしくは要注意構造を持つ遺伝毒性物質の幾つかについて高い発がんリスクを懸念している．[2] このため，多くの専門家は食事中に低レベルで存在する遺伝毒性／要注意構造を持つ発がん物質に関しては TTC を 1 桁低い 0.15 μg/人とすることを推奨している．さらに，TTC が適応できないような極めて強力な遺伝毒性発がん物質としてアフラトキシン類，アゾキシ化合物，ニトロソ化合物を挙げている．これら化合物に関しては個別の毒性データとリスク管理が必要であり，TTC を適用すべきではない．

一方，医薬品に関しては別の TTC の考え方がある．医薬品そのものに遺伝毒性があることは許されないが，そこに含まれる不純物に遺伝毒性がある場合，TTC の概念を取り入れた不純物のリスク管理が米国，EU でガイドライン化されつつある．これらガイドラインでは場合によっては，不純物に遺伝毒性があっても 1 日あたり 120 μg/人までの TTC が許容される．医薬品は食事と異なり，摂取(服用)期間が限られていること，また医薬品のベネフィットを考慮した 10^{-5} のリスクレベルなどが採用された段階的 TTC が提唱されている．[3]

6 おわりに

発がん率は人口あたりで発生するがん患者の数であり，動物実験による発がん性試験は担がん動物の数によって評価される．その単位は/人口，/動物数であり普遍である．一方，遺伝毒性の単位は試験系によって異なる．エームス試験は/plate，染色体異常試験は/cell，遺伝子突然変異試験は/gene によって評価される．単位が違えばその検出レベルも異なり，そこで仮に閾値が観察されたとしても，その値は試験系に依存する．また，発がん性は種差，個体差等によって変動することは当然考えられるが，遺伝毒性とは「DNA や染色体の構造的もしくは量的変化を引き起こす性質」であり，DNA や染色体がすべての生物で共通であることを考慮すると，それは普遍でなくてはならない．もし，遺伝毒性に閾値が存在するのであれば，試験法によってそれが変動すること自体が矛盾である．したがって，遺伝毒性とはそもそも閾値を論じるような性質のものではないといえるのかも知れない．

遺伝毒性発がん物質に無理に閾値を設定し，ゼロリスクを求めるよりも，低レベルのリスクを，無視しうる(negligible)，もしくは許容できる(acceptable)リスクとして評価し，社会が受け入れることの方が現実的と考える．文明社会で生活する限り，多くの化学物質の摂取は不可避であり，そのベネフィットとリスクのバランスを考えることが重要である．また，我々人間は自然の食物からも多くの化学物質を摂取しており，それらが遺伝毒性発がん物質であることも少なくない．これら化学物質の中には，一般化学物質よりも高い 10^{-4}～10^{-5} というリスクレベルでないと管理できないものもある．Doll と Peto が言うようにがんの最大の原因は我々の日常の食べ物にあり，残留農薬や食品添加物にあるのではない．[4] もちろん，これらリスクはできるだけ回避することは必要であるが，やはりここでもバランスが重要である．このバランス感覚を身につけることが，成熟した社会での安心した生活に繋がるものと考える．

参考文献

1) Cheeseman M. *et al*., *Food Chem. Toxicol*., 37, 387–412 (1999).
2) Kroes R. *et al*., *Food Chem. Toxicol*., 42, 65–83 (2004).
3) Muller L. *et al*., *Regul. Toxicol. Pharmacol*., 44, 198–211 (2006).
4) Doll R., Peto R., "The Cause of Cancer," Oxford University Press, 1982

DNA REPAIR 7 (2008) 663–669

available at www.sciencedirect.com

ScienceDirect

journal homepage: www.elsevier.com/locate/dnarepair

DNA Repair

Brief report

Mutagenesis of uracil-DNA glycosylase deficient mutants of the extremely thermophilic eubacterium *Thermus thermophilus*

*Tomoya Sakai, Shin-ichi Tokishita, Kayo Mochizuki, Ayako Motomiya, Hideo Yamagata, Toshihiro Ohta**

School of Life Sciences, Tokyo University of Pharmacy and Life Sciences, 1432-1 Horinouchi, Hachioji, Tokyo 192-0392, Japan

ARTICLE INFO

Article history:
Received 20 September 2007
Received in revised form
7 January 2008
Accepted 14 January 2008

Keywords:
Uracil-DNA glycosylase
Thermus thermophilus
Mutator
Bgl assay

ABSTRACT

Thermus thermophilus is an extremely thermophilic, aerobic, and gram-negative eubacterium that grows optimally at 70–75 °C, pH 7.5. In extremely high temperature environment, DNA damages in cells occur at a much higher frequency in thermophiles than mesophiles such as *E. coli*. When temperature rises, the deamination of cytosine residues in double-strand DNA is expected to increase greatly. *T. thermophilus* HB27 has two putative uracil-DNA glycosylase genes (*udgA* and *udgB*). Expression level of *udgA* gene was 2–3 times higher than that of *udgB* at 70, 74, and 78 °C when it was monitored by β-glucosidase reporter assay. We developed $hisD_{3110}$, $hisD_{3113}$, $hisD_{3115}$, and $hisD_{174}$ marker allele that can specifically detect G:C → A:T, C:G → A:T, T:A → A:T, and A:T → G:C base-substitutions, respectively, by His$^+$ reverse mutations. We then disrupted *udgA* and *udgB* by thermostable kanamycin-resistant gene (*htk*) or *pyrE* gene insertion in each *hisD* background, and their spontaneous His$^+$ reversion frequencies were compared. A *udgA,B* double mutant showed a pronounced increase in G:C → A:T reversion frequency compared with each single *udg* mutant, *udgA* or *udgB*. Estimated mutation rates of the *udgA,B* mutant cultured at 60, 70, and 78 °C were about 2, 12, and 117 His$^+$/10^8/generation, respectively. At 70 °C culture, increased ratio of the mutation rate compared with the *udg*$^+$ strain was 12-fold in *udgA*, 3-fold in *udgB*, and 56-fold in *udgA,B* mutant. On the other hand, no difference was observed in other mutations of C:G → A:T, T:A → A:T, and A:T → G:C between *udgA,B* double mutant and the parent *udg*$^+$ strain. The present results indicated that gene products of *udgB* as well as *udgA* functioned in vivo to remove uracil in DNA and prevent G:C → A:T transition mutations.

1. Introduction

Thermus thermophilus HB27, isolated from a Japanese thermal spa, is an extremely thermophilic eubacterium that grows at 55–82 °C [1]. It is a nonsporulating, gram-negative, aerobic, obligate heterotroph that grows optimally at 70–75 °C and pH 7.5. Because of the rapid growth rate of *T. thermophilus* and the ease of purifying its proteins, its thermostable enzymes have been extensively studied in vitro, including in a structural genomics project [2]. The genome of the strain HB27

* *Corresponding author*. Tel.: +81 42 676 7093; fax: +81 42 676 7081.
E-mail address: ohta@ls.toyaku.ac.jp (T. Ohta).
1568-7864/$ – see front matter © 2008 Elsevier B.V. All rights reserved.
doi:10.1016/j.dnarep.2008.01.006

has been sequenced [3] and consists of about 2200 putative genes divided between a 1.89 Mbp chromosome and a 0.23 Mbp megaplasmid (pTT27). *T. thermophilus* shows natural transformation competence throughout its growth phase with efficiency on the order of 10^4 transformants/μg DNA [4]. Although available antibiotic resistance genes at 70 °C are limited, a host–vector system was developed using the cryptic plasmid pTT8 (copy number: 8/cells) with a thermostable kanamycin-resistant *htk* gene [5]. On the other hand, a chemically defined medium for HB27 has been developed [6]. It provides a genetic method using auxotroph mutants.

Our major interest is DNA repair systems that function in extremely high temperature environments and the mechanisms of mutagenesis in *T. thermophilus*, because we would expect endogenous DNA damage such as deamination, depurination, methylation, oxidation, and single strand breaks to occur at a much higher frequency in thermophiles than in mesophiles. The spontaneous hydrolytic deamination of cytosine to uracil occurs frequently in the intracellular environment. A mismatched base pair G:U resulting from cytosine deamination generates an A:U base pair after replication. Subsequent replication of an A:U base pair should result in G:C → A:T transition mutation [7,8]. To prevent the occurrence of mutations by uracil in DNA, a base excision repair pathway has an important role [9]. Uracil-DNA glycosylase (UDG) catalyzes the first step in the repair pathway for uracil-containing DNA. The enzyme releases uracil from DNA by hydrolyzing the bond between the base and a deoxyribose [10]. Based on the amino acid sequences similarity and differences in substrate specificity, UDGs are classified into five families [9,11]. Family 1 UDGs (Ung family) excise uracil base from single-stranded DNA and double-stranded DNA. *E. coli* Ung is the representative of this family. Family 1 UDGs are found in many organisms including bacteria, yeast, mammalian cells, and plant cells, but not in archaea and insects. Family 2 UDGs (Mug/TDG family) consist of bacterial mismatch-specific uracil-DNA glycosylases (Mug) [12] and eukaryotic thymine-DNA glycosylases (TDG) [13,14]. They remove 3, N^4-ethenocytosine as well as uracil when mispaired with guanine. It has been reported that *E. coli* mug mutant showed no effect on G:C → A:T mutations [15]. Therefore, the principal role of family 2 UDGs may be the removal of 3, N^4-ethenocytosine. Family 3 UDGs (SMUG family) are single-strand-specific monofunctional uracil-DNA glycosylases (SMUG) and are identified in vertebrates and insects. They act on uracil and 5-hydroxymethyluracil in DNA [16]. Quite recently a bacterial SMUG ortholog has been reported in *Geobacter metallireducens* [17]. Family 4 UDGs (TmUDG) are thermostable UDG family found in thermophilic archaea and bacterial species. *Thermotoga maritima* UDG (TmUDG) is the representative of this family [18]. Family 4 enzymes from hyperthermophile archaea *Archaeoglobus fulgidus* [19] and *Pyrobaculum aerophilum* [20] are also characterized. They remove uracil from duplex DNA and single-stranded DNA containing uracil. Family 5 UDGs (UDG-b family) are found only in hyperthermophilic archaeon *P. aerophilum* [21] and eubacterium *T. thermophilus* [22]. They act on uracil in duplex DNA. PaUDG also catalyzes the removal of hypoxanthine, a product of adenine deamination. This enzyme, therefore, may play an important role against deamination of both cytosine and adenine. In addition to the above five UDG families, a novel UDG has been identified from hyperthermophilic archaeon *Methanococcus jannaschii* [23]. The MjUDG catalyzes the excision of 8-hydroxyguanine as well as uracil from DNA.

T. thermophilus HB27 has two putative UDG genes, *udgA* (TTC0366) and *udgB* (TTC0784) [22]. The former belongs to the family 4 UDGs and the latter is the family 5 UDGs. Since there is no report on isolation and characterization of *udg*-deficient mutants of *T. thermophilus*, little is known about the function and complementation of the two genes in vivo at growing temperature. We first investigated expression level of the *udgA* and *udgB* genes at different temperature by a newly developed β-glucosidase (Bgl) reporter assay. We demonstrate the constitutive expression of both the genes. Then, we developed a set of *hisD* reverse mutation assay system to determine the mutation spectrum and used it to investigate mutator phenotype of *udg* mutants. We report here the evidence that gene products of *udgB* as well as *udgA* functioned in vivo to prevent G:C → A:T transition mutations.

2. Materials and methods

2.1. Bacterial strains, culture media, and chemicals

Table 1 shows the strains of *T. thermophilus* used in this study. Bacteria were cultured in PY medium (0.8% polypeptone, 0.4% Difco yeast extract, 0.2% NaCl, 0.35 mM $CaCl_2$, and 0.4 mM $MgCl_2$) at 70 °C with shaking. MSG minimal medium (pH 7.5) consisted of 2% sucrose, 2% sodium glutamate, 0.2% NaCl, 0.05% $(NH_4)_2SO_4$, 0.05% K_2HPO_4, 0.025% KH_2PO_4, 88 μg/ml $CaCl_2{\cdot}2H_2O$, 35 μg/ml $MgCl_2{\cdot}6H_2O$, 1.2 μg/ml $Na_2MoO_4{\cdot}2H_2O$, 0.5 μg/ml $MnCl_2{\cdot}4H_2O$, 0.1 μg/ml $VOSO_4{\cdot}nH_2O$, 0.06 μg/ml $ZnSO_4{\cdot}7H_2O$, 0.08 μg/ml $CoCl_2{\cdot}6H_2O$, 0.015 μg/ml $CuSO_4{\cdot}5H_2O$, 0.002 μg/ml $NiCl_2{\cdot}6H_2O$, 6.7 μg/ml $FeSO_4{\cdot}7H_2O$, 0.1 μg/ml biotin, and 1 μg/ml thiamine. Medium was solidified with 1.5% agar for culture at 70 °C or 1.5% gellan gum for culture at 74 °C. Top agar contained 0.6% agar without NaCl. *Escherichia coli* strain XL1-Blue MRF' and vector plasmids pCR4-TOPO (Invitrogen Japan K.K., Tokyo) were used for plasmid construction. Gellan gum, 5-fluoroorotic acid (FOA), and 2-nitrophenyl-β-D-glucopyranoside (2NPGlc) were obtained from Wako Pure Chemical Industry, Tokyo. Kanamycin sulfate was purchased from Sigma–Aldrich Co., MO, USA.

2.2. Construction of $hisD_{3110}$, $hisD_{3113}$, and $hisD_{3115}$ mutation allele

The *hisD* gene encodes the enzyme L-histidinol dehydrogenase. The active site residue His-327 in PEHL motif of *E. coli* HisD protein participates in acid–base catalysis, whereas Glu-326 is responsible for the activation of a water molecule [24]. Since the corresponding Glu-311 in PEHL motif of *T. thermophilus* HisD protein would be expected to be indispensable for catalytic activity, we substituted the amino acid to obtain His auxotroph mutants. About 1800 bp fragment containing *hisD* was amplified by PCR from HB27 DNA and cloned onto pCR4-TOPO. GAG codon for Glu-311 in *hisD* gene was changed to GGG, GCG, or GTG codon for Gly, Ala, and Val, respectively, by site-directed mutagenesis. The HB27 cells were transformed

Table 1 – *Thermus thermophilus* strains used in this study

Strain	Genotype	Source/construction
HB27	wild-type	A. Yamagishi
RT30	$hisD_{3110}$	Mutation at ^{311}Glu (GAG) to Gly (GGG), His^+ reversion by G:C to A:T transition
TS7	$hisD_{3110}$, Δ*pyrE*	RT30 × pKN605 (Δ*pyrE*), FOA^r
AYA31	$hisD_{3110}$, *udgA::htk*	RT30 × pHTK366 (*udgA::htk*), Km^r
AYA22	$hisD_{3110}$, *udgB::pyrE*	TS7 × pURA784 (*udgB::pyrE*), Ura^+
AYA55	$hisD_{3110}$, *udgA::htk*, *udgB::pyrE*	AYA22 × pHTK366 (*udgA::htk*), Km^r
RT40	$hisD_{3113}$	Mutation at ^{311}Glu (GAG) to Ala (GCG), His^+ reversion by C:G to A:T transversion
TS17	$hisD_{3113}$, Δ*pyrE*	RT40 × pKN605 (Δ*pyrE*), FOA^r
TS298	$hisD_{3113}$, *udgB::pyrE*	TS17 × pURA784 (*udgB::pyrE*), Ura^+
TS308	$hisD_{3113}$, *udgA::htk*, *udgB::pyrE*	TS298 × pHTK366 (*udgA::htk*), Km^r
RT50	$hisD_{3115}$	Mutation at ^{311}Glu (GAG) to Val (GTG), His^+ reversion by T:A to A:T transversion
TS27	$hisD_{3115}$, Δ*pyrE*	RT50 × pKN605 (Δ*pyrE*), FOA^r
TS398	$hisD_{3115}$, *udgB::pyrE*	TS27 × pURA784 (*udgB::pyrE*), Ura^+
TS408	$hisD_{3115}$, *udgA::htk*, *udgB::pyrE*	TS398 × pHTK366 (*udgA::htk*), Km^r
WH11	$hisD_{174}$	Mutation at ^{174}Gly (GGG) to Glu (GAG), His^+ reversion by A:T to G:C transition [25]
MS8	$hisD_{174}$, Δ*pyrE*	WH11 × pKN605 (Δ*pyrE*), FOA^r
KM709	$hisD_{174}$, *udgB::pyrE*	MS8 × pURA784 (*udgB::pyrE*), Ura^+
KM754	$hisD_{174}$, *udgA::htk*, *udgB::pyrE*	KM709 × pHTK366 (*udgA::htk*), Km^r
JOS9	Δ*bgl*	[26]

by homologous recombination with the mutated *hisD* gene fragment on linearized plasmid. His auxotroph mutants were isolated by replica plating method on MSG plates with and without 100 μg/ml His. Introduction of the mutation allele ($hisD_{3110}$ in RT30, $hisD_{3113}$ in RT40, and $hisD_{3115}$ in RT50) in the His auxotroph colonies was confirmed by DNA sequencing. Then 56, 58 and 52 His^+ spontaneous revertants were isolated from RT30, RT40, and RT50, respectively, to determine their base-substitutional event. All the His^+ revertants restored GAG (Glu) codon from GGG (Glu) in RT30, GCG (Ala) in RT40 or GTG (Val) in RT50. No other base-substitutions such as AGG (Arg), TGG (Trp), CGG (Arg), ACG (Thr), CCG (Pro), and TCG (Ser) were found. Therefore, induction of G:C → A:T, C:G → A:T, and T:A → A:T base-substitutions could be specifically detected in the strain RT30, RT40, and RT50, respectively, by His^+ reverse mutations. On the other hand, $hisD_{174}$ allele in WH11 has been identified as a codon change from Gly-174 (GGG) to Glu (GAG) and induction of A:T → G:C transitions could be specifically detected at the target site in our previous study [25].

2.3. *Gene disruption by insertion of htk or pyrE gene cassette*

pKN605 carrying TTC1379-(Δ*pyrE*)-TTC1381 genes and p3TSDN2 carrying the *pyrE* gene cassette (0.6 kbp) were gifts of Dr. M. Tamakoshi (Tokyo University of Pharmacy and Life Science, Japan). An *htk* gene cassette including the promoter region (1.0 kbp) was amplified by PCR from pTAP60 [26] using primers having a *Sac*I site. DNA repair genes (*udgA* and *udgB*) were amplified by PCR from HB27 genomic DNA and subcloned into the plasmid pCR4-TOPO. Then the *Hin*dIII restriction site was incorporated upstream of the *Bam*HI site in the *udgB* gene by PCR for the insertion of the *pyrE* gene fragment. The *htk* gene fragment was inserted into the *Sac*I site in the middle of the *udgA* gene. Transformation of *E. coli* XL1-Blue with the ligated plasmid yielded pHTK366 (*udgA::htk*) and pURA784 (*udgB::pyrE*).

2.4. *Transformation*

Plasmids pHTK366 and pURA784 linearized by *Spe*I or *Nco*I digestion were used for transformation of the *T. thermophilus* strains. A logarithmic growing cell culture (0.5 ml) in PY medium at 70 °C (approx. 1×10^8 cells/ml) was mixed with 25–50 μl of the linearized plasmid DNA solution and cultured for 2 h at 70 °C with gentle shaking to allow homologous recombination. A portion of the culture was spread on PY plates containing 50–100 μg/ml of kanamycin for the selection of transformants containing the *htk* gene. For the selection of $pyrE^+$ (Ura^+) and Δ*pyrE* (Ura^-, FOA^r) transformants, cells were washed with Na–phosphate buffer (10 mM, pH 7.4) by centrifugation and spread on MSG plate supplemented, respectively, with 100 μg/ml His or 100 μg/ml His, 50 μg/ml uracil, and 500 μg/ml FOA. Plates were wrapped in PVC wrapping film and incubated 1–3 days at 70 °C for colony formation. A band of expected size of *udgA::htk* (or *udgB::pyrE*) was amplified by PCR from Km^r (or Ura^+) clone, whereas a band of the original size of *udgA* (or *udgB*) was not detected, indicating that the *udgA* (or *udgB*) gene was correctly replaced with *uvrB::htk* (or *udgB::pyrE*) by homologous recombination.

2.5. *Spontaneous His^+ reversion frequency*

Independent single colony grown on PY agar plate for 2 days was inoculated into fresh PY medium (OD_{600} = 0.1–0.2) and cultured at 70 °C for additional 4–5 h with shaking (OD_{600} = 0.8–1.6). Cells were washed with Na–phosphate buffer and suspended in buffer at OD_{600} = 1.0. For the measurement of His^+ mutants, 0.3 ml was plated onto triplicate MSG plates with 2 ml of top agar. For the determination of viable cells, after 10^{-6} dilution, 0.1-ml was plated onto triplicate PY plates with 2 ml of top agar. Plates were incubated for 2–3 days for MSG plates and 1–2 days for PY plate at 70 °C. Experiments were repeated 3–4 times and total 9 or 13 independent cultures were determined for their mutation frequency.

Mutation rates (His$^+$/10^8/generation) in RT30, AYA31, AYA22, and AYA55 were measured at different growth temperatures, 60, 70, and 78 °C. Bacterial cells grown overnight at 60 °C (OD_{600} = 1.64–2.47) were diluted 1/40-fold with fresh PY medium and cultured at 60, 70, and 78 °C for 8, 6, and 6 h, respectively. The mean number of cell division (n) was calculated from the values of OD_{600}. His$^+$ mutation frequency (His$^+$/10^8) was measured before and after the cultivation by the method described above using 5 MSG plates for His$^+$ cells and 5 PY plates for viable cells. All the plates were incubated at 70 °C for colony formation. Mutation rate at 78 °C (MR_{78}) was calculated as MR_{78} = {(His$^+$/10^8 at 78 °C)—(His$^+$/10^8 in preculture at 60 °C)}/n. MR_{70} and MR_{60} were similarly determined. Experiments were conducted twice.

2.6. *Bgl assay*

The plasmid vector pGLS1531 for β-glucosidase (Bgl) reporter assay was described previously [26]. The 5′-upstream region of the *udgA* gene (TTC0366) or the *udgB* gene (TTC0784) was amplified from HB27 chromosomal DNA using PCR primers having 5′-*Aor*13HI and 3′-*Hin*dIII sites. Plasmids pGLS366-1 (*udgA′-bgl*), pGLS366-2 (TTC0367-*udgA′-bgl*), pGLS784-1 (*udgB′-bgl*), and pGLS784-2 (*pccB-udgB′-bgl*) were constructed by replacing the *Aor*13HI-*Hin*dIII region of pGLS1531 with the PCR fragment. Plasmids were introduced into JOS9 (Δ *bgl*) by selection of a Km^r transformant. Bacterial cells were cultured overnight at 70, 74, or 78 °C in PY medium. Bgl activity of toluenized cells was assayed at 80 °C with 2NPGlc as a substrate [26]. Experiments were repeated 3–4 times and mean values were presented in the figures.

3. Results

3.1. *Expression of udgA and udgB genes*

The expression of *udgA* and *udgB* genes was investigated with Bgl reporter assay. It is likely that the *udgA* gene is organized in an operon-like structure with adjacent upstream hypothetical gene TTC0367, because Bgl activity was detected for pGLS366-2 (TTC0367-*udgA′-bgl*) including 5′-upstream region of TTC0367, but not for pGLS366-1 (*udgA′-bgl*) without the region as shown in Fig. 1. Also the *udgB* gene forms an operon-like structure with its upstream gene, *pccB*, because pGLS784-1 (*udgB′-bgl*) lacking 5′-upstream region of *pccB* revealed no Bgl activity (Fig. 1). The *pccB* gene encodes propionyl-CoA carboxylase beta chain, but the functional correlation with the repair gene *udgB* is not known. Gene expression was almost same level between 70 and 74 °C, but it was decreased at 78 °C, an over-optimal temperature (Fig. 2). The expression levels of *udgA* were about 1.8, 2.4, and 3.4 times that of *udgB* at 70, 74, and 78 °C, respectively. We also investigated the effect of temperature shift-up on the expression of *udgA* and *udgB* genes. An overnight culture at 60 °C was transferred into fresh PY medium and cultured at 70, 74, and 78 °C for 30, 60 and 90 min. Obvious changes in Bgl activity were not observed under the condition, suggesting constitutive gene expression (data not shown).

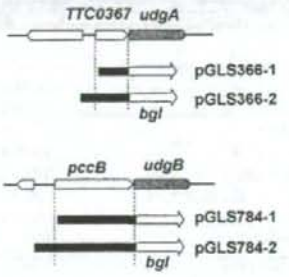

plasmid (JOS9)	Bglactivity (unit/OD600) mean ± SD
–	0.22 ± 0.16
pGLS366-1	0.19 ± 0.04
pGLS366-2	2.34 ± 0.12**
pGLS784-1	0.18 ± 0.06
pGLS784-2	1.47 ± 0.17**

Fig. 1 – Expression of *udgA* and *udgB* gene. Bgl activity was measured for JOS9 (Δ*bgl*) with and without each plasmid. Data are the means of three experiments. The left panel shows a part of *T. thermophilus* genome and the regions of insertion (black bar) into a *bgl* vector. Statistically significant from JOS9 (without plasmid) at $P < 0.01$ (**) by the Dunnett test.

3.2. *Spontaneous hisD reversion frequency*

Two UDG genes, *udgA* and *udgB*, were disrupted by the insertion of *htk* or *pyrE* in 4 different background, $hisD_{174}$, $hisD_{3110}$, $hisD_{3113}$, and $hisD_{3115}$. Deletion of both *udgA* and *udgB* gene was not lethal. Neither obvious growth delay in PY liquid medium nor decrease in colony-forming ability on PY plate of *udgA,B* double mutant was observed at 70 and 74 °C (data not shown). To measure the effect of the *udg* mutation on the frequency of various spontaneous base-substitution mutations, we used the *hisD* reversion system. Spontaneous His$^+$ mutation frequencies of *udg*-deficient strains were compared with corresponding parent strain WH11, RT30, RT40, or RT50. Concerning the G:C→A:T transitions, the $hisD_{3110}$ reversion frequency of AYA31 (*udgA*) was about 14.7 times that of RT30, while that of AYA22 (*udgB*) was 2.7-fold increase compared with RT30 (Fig. 3). The *udgB* mutant showed weak mutator effect. In contrast to the single *udg* mutant, a pronounced increase in reversion frequency was observed in a double mutant strain AYA55 (*udgA, udgB*). It was about 81.6 times that of RT30. When it was compared between AYA31 (*udgA*)

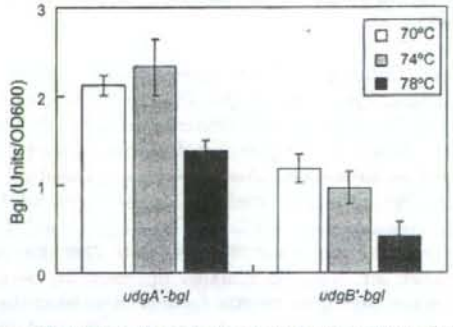

Fig. 2 – Effect of growth temperature on the *udgA* and *udgB* gene expression. JOS9 (Δ*bgl*) cells carrying pGLS366-2 (*udgA′-bgl*) or pGLS784-2 (*udgB′-bgl*) were cultured overnight at 70, 74, or 78 °C. Data are the means of four experiments.

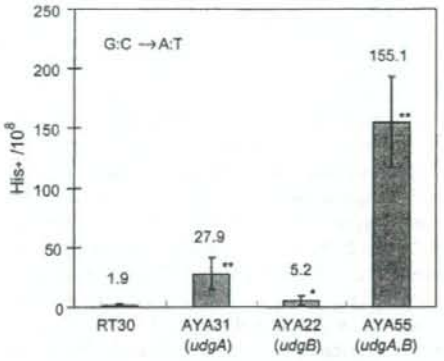

Fig. 3 – Spontaneous mutation frequency of $his D_{3110}$ reversion (G:C → A:T) in *udg* mutants. Values are the mean of 13 independent cultures. Statistically significant from RT30 at $P<0.05$ (*) or $P<0.01$ (**) by the Kruskal Wallis test.

and AYA55 (*udgA*, *udgB*), about 5.6-fold increase was observed. The difference would provide the evidence of UdgB activity in a *udgA* background. The results indicated that *udgB* as well as *udgA* gene product played an important role to prevent G:C → A:T transition mutations. Since uracil residues in DNA would not be expected to increase the mutation frequency other than G:C → A:T transitions, we further measured the spontaneous His$^+$ reversion frequencies of *udgA,B* mutants in $his D_{174}$, $his D_{3113}$, or $his D_{3115}$ background. For A:T → G:C transitions, the reversion frequencies of WH11 and KM754 (*udgA,B*) were 0.77 ± 0.59 and $1.22 \pm 0.82 \times 10^{-8}$, respectively (Fig. 4). For C:G → A:T transversions, those of RT40 and TS308 (*udgA,B*) were 3.07 ± 1.22 and $2.24 \pm 2.16 \times 10^{-8}$, respectively. Also those of RT50 and TS408 (*udgA,B*) for T:A → A:T transversions were 1.40 ± 0.63 and $2.02 \pm 1.40 \times 10^{-8}$, respectively. In each comparison, statistical differences were not observed. Thus, deletion of *udgA,B* did not alter the reversion frequencies of the $his D_{174}$, $his D_{3113}$, and $his D_{3115}$ allele as shown in Fig. 4.

As far as investigated, frequency of only G:C → A:T transitions was elevated by the deficiency of *udgA,B* genes. We,

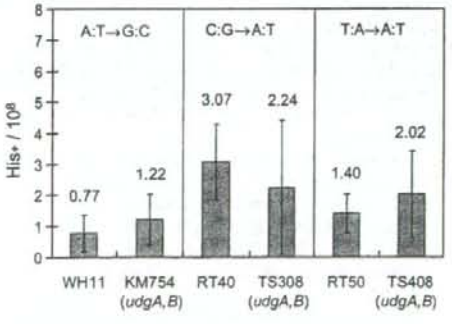

Fig. 4 – Spontaneous mutation frequency of $his D_{174}$ reversion (A:T → G:C), $his D_{3113}$ reversion (C:G → A:T), and $his D_{3115}$ reversion (T:A → A:T) in *udgA,B* mutants and their parent strains. Values are the mean of nine independent cultures.

Table 2 – Mutation rates of G:C to A:T transitions in *udg* mutants cultured at different temperatures

Strain	60 °C culture (start)		Cultured at 60 °C for 8 h					Cultured at 70 °C for 6 h					Cultured at 78 °C for 6 h				
	OD_{600}	His$^+$/10^8	OD_{600}	His$^+$/10^8	n	MR_{60}	Ratio	OD_{600}	His$^+$/10^8	n	MR_{70}	Ratio	OD_{600}	His$^+$/10^8	n	MR_{78}	Ratio
RT30	0.057	0.32	1.12	0.44	4.3	0.028		1.80	1.31	5.0	0.20		1.25	5.05	4.5	1.05	
udg$^+$	0.042	1.28	0.80	1.71	4.3	0.10 (0.064)	1	0.97	2.25	4.5	0.22 (0.21)	1	0.92	28.72	4.5	6.10 (3.58)	1
AYA31	0.041	9.90	0.92	11.59	4.5	0.38		1.03	27.44	4.7	3.73		0.70	53.29	4.1	10.58	
udgA	0.040	6.59	0.96	8.61	4.6	0.44 (0.41)	6.4	1.04	13.15	4.7	1.40 (2.57)	12.2	0.92	42.01	4.5	7.87 (9.23)	2.6
AYA22	0.052	0.44	1.03	1.09	4.5	0.14		0.89	4.58	4.7	0.88		0.79	18.64	4.1	4.44	
udgB	0.057	2.93	0.99	3.48	4.6	0.12 (0.13)	2.0	1.15	4.39	4.7	0.31 (0.60)	2.9	0.79	20.85	4.5	3.98 (4.21)	1.2
AYA55	0.062	89.72	1.05	102.70	4.1	3.17		1.01	154.50	4.1	15.80		0.60	524.20	3.2	135.78	
udgA,B	0.048	43.25	0.86	48.04	4.2	1.14 (2.15)	33.6	1.27	79.26	4.7	7.66 (11.73)	55.9	1.14	495.75	4.6	98.37 (117.1)	32.7

Bacterial cultures at 60 °C were diluted 1/40-fold with fresh PY medium and cultured at 60, 70, and 78 °C for 8, 6, and 6 h, respectively. The mean number of cell division (n) was calculated from the values of OD_{600}. MR_{60}, MR_{70}, and MR_{78} represent the mutation rates (His$^+$/10^8/generation) at 60, 70, and 78 °C, respectively. Data of two independent experiments were presented. Values in parentheses were the mean of two experiments.

therefore, further investigated mutation rates in strains RT30, AYA31, AYA22, and AYA55 at different growth temperatures. Cells grown at 60 °C were inoculated into PY medium and cultured at 60, 70, and 78 °C for 6–8 h. The estimated mutation rates of G:C → A:T transitions in *udg*-proficient strain RT30 were 0.064, 0.21, and 3.58 $His^+/10^8$/generation, respectively, at 60, 70, and 78 °C (Table 2). In the absence of *udgA* gene function, they were 0.41, 2.57, and 9.23 $His^+/10^8$/generation at 60, 70, and 78 °C, respectively. Similar temperature-dependent increase in mutation rate was observed in *udgB* strain AYA22. At any temperature the mutation rates were lower than those in *udgA* strain AYA31. Compared with the single mutants, higher mutation rates were observed in AYA55 (*udgA,B*). Their mutation rates at 60, 70, and 78 °C were estimated to be 2.15, 11.73, and 117.1 $His^+/10^8$/generation, respectively. At 70 °C culture, increased ratio of the mutation rate (RT_{70}) compared with the *udg*$^+$ strain was about 12-fold in *udgA*, 3-fold in *udgB*, and 56-fold in *udgA,B* strain. These values were almost same degree as those observed in Fig. 3.

4. Discussion

Deamination of the normal DNA base cytosine to form uracil is one of the major endogenous DNA damages. If the uracil base is not removed before replication, it causes G:C → A:T transition mutations [7]. A mutant of *E. coli* deficient in UDG activity shows an increased rate of spontaneous G:C → A:T mutations [8]. The UDG enzyme system seems to be the universal mechanism for uracil repair, since UDG-homologous genes can be found in a variety of organisms including bacteria, viruses, and eukaryotes. The spontaneous deamination reaction is greatly enhanced at high temperature and, therefore, formation of U:G pre-mutagenic mispair caused by cytosine deamination is particularly profound for extreme thermophiles. Thus, it is plausible that they may have more effective repair systems compared with other mesophiles. *T. thermophilus* has two UDGs, termed UdgA and UdgB. Starkuviene and Fritz [22] reported that UdgA protein belongs to the family of thermostable UDGs and catalyzes the removal of uracil from duplex DNA and single-stranded DNA containing uracil. On the other hand, UdgB, a novel family 5 UDGs, acted on uracil residues in duplex DNA, but not in single-stranded DNA. However, these in vitro assays were performed at 50 °C. It is not known whether these Udg proteins exhibit their enzyme activity at 70 °C or higher. Hoseki et al. [27] have reported crystal structure analysis of UdgA that it removed uracil from DNA in the same manner as did family 1 UDGs. In contrast to the in vitro studies on purified UdgA and UdgB proteins, the role of two enzymes in counteracting the mutagenic threat of cytosine deamination has not been elucidated in vivo at growing temperature.

In the present study, we demonstrated that both the UdgA and UdgB glycosylases prevented mutations caused by cytosine deamination in *T. thermophilus*. MR_{70} of G:C → A:T transitions was stimulated about 56-fold in the *udgA,B* double mutant strain compared with the *udg*$^+$ strain, and about 4.6-fold compared with the *udgA* strain (Table 2). The MR_{70} in *udgB* strain was about 3 times that in the *udg*$^+$ strain. The difference between *udgA* and *udgA,B* strains indicated the function of *udgB* gene in repair of uracil. It is evident that a UdgB glycosylase actually functions in vivo. The temperature-dependent increase in mutation rate in any strain would indicate the enhancement of cytosine deamination at high temperature. Since MR_{78} in the *udg*$^+$ strain was greatly enhanced compared with MR_{70}, repair efficiency of the UdgA and UdgB would be decreased at 78 °C, an over-optimal temperature. It is consistent with the observation that gene expression of *udgA* and *udgB* was also decreased at 78 °C (Fig. 2). Both of the genes seemed to be expressed constitutively. It is unlikely that UdgB acts at higher temperature. On the other hand, other base-substitutions were not affected by the introduction of *udgA,B* mutations. We have not developed other two *hisD* allele for the detection of G:C → C:G and A:T → C:G transversions. However, these types of mutations are known to be comparatively rare event among the base-substitutions found in *E. coli* and *Salmonella typhimurium* [28,29]. Lack of a mismatch repair function (*mutL,H,S*) stimulates G:C → A:T and A:T → G:C transitions, whereas inactivation of repair enzymes for 8-hydroxyguanine (*mutM,Y*) enhances specifically C:G → A:T transversions in *E. coli* [9]. Our *hisD* reversion system developed in the present study would be useful for the investigation of gene functions such as *mutS*, *mutS2*, *mutL*, *mutM*, and *mutY* on mutagenesis in *T. thermophilus*.

Acknowledgments

We thank Drs. Akihiko Yamagishi and Masatada Tamakoshi, Tokyo University of Pharmacy and Life Sciences, for providing bacterial strain HB27 and plasmids. We also thank Rumi Tsunoi for her technical assistance. This work was supported in part by Grants-in Aid for Scientific Research from the Ministry of Education, Science, Sports, and Culture of Japan.

REFERENCES

[1] T. Oshima, K. Imahori, Description of *Thermus thermophilus* (Yoshida and Oshima) comb. nov., a nonsporulating thermophilic bacterium from a Japanese thermal spa, Int. J. Syst. Bacteriol. 24 (1974) 102–112.

[2] S. Yokoyama, Y. Matsuo, H. Hirota, T. Kigawa, M. Shirouzu, Y. Kuroda, H. Kurumizaka, S. Kawaguchi, Y. Ito, T. Shibata, M. Kainosho, Y. Nishimura, Y. Inoue, S. Kuramitsu, Structural genomics projects in Japan, Prog. Biophys. Mol. Biol. 73 (2000) 363–376.

[3] A. Henne, H. Bruggemann, C. Raasch, A. Wiezer, T. Hartsch, H. Liesegang, A. Johann, T. Lienard, O. Gohl, R. Martinez-Arias, C. Jacobi, V. Starkuviene, S. Schlenczeck, S. Dencker, R. Huber, H.P. Klenk, W. Kramer, R. Merkl, G. Gottschalk, H.J. Fritz, The genome sequence of the extreme thermophile *Thermus thermophiles*, Nat. Biotechnol. 22 (2004) 547–553.

[4] Y. Koyama, T. Hoshino, N. Tomizuka, K. Furukawa, Genetic transformation of the extreme thermophilic *Thermus thermophilus* and of other *Thermus* spp., J. Bacteriol. 166 (1986) 338–340.

[5] Y. Koyama, Y. Arikawa, K. Furukawa, A plasmid vector for an extreme thermophile, *Thermus thermophiles*, FEMS Microbiol. Lett. 72 (1990) 97–102.

[6] T. Oshima, M. Baba, Occurrence of *sym*-homospermidine in extremely thermophilic bacteria, Biochem. Biophys. Res. Commun. 103 (1981) 156–160.
[7] B.K. Duncan, J.H. Miller, Mutagenic deamination of cytosine residues in DNA, Nature 287 (1980) 560–561.
[8] B.K. Duncan, B. Weiss, Specific mutator effects of *ung* (uracil-DNA glycosylase) mutations in *Escherichia coli*, J. Bacteriol. 151 (1982) 750–755.
[9] E.C. Friedberg, G.C. Walker, W. Siede, R.D. Wood, R.A. Schultz, T. Ellenberger (Eds.), Base excision repair. In: DNA Repair and Mutagenesis, second ed., ASM Press, Washington, DC, 2006, pp. 169–226.
[10] T. Lindahl, An N-glycosylase from *Escherichia coli* that releases free uracil from DNA containing deaminated cytosine residues, Proc. Natl. Acad. Sci. U.S.A. 71 (1974) 3649–3653.
[11] L.H. Pearl, Structure and function in the uracil-DNA glycosylase superfamily, Mutat. Res. 460 (2000) 165–181.
[12] P. Gallinari, J. Jiricny, A new class of uracil-DNA glycosylases related to human thymine-DNA glycosylase from HeLa cells, Nature 383 (1996) 735–738.
[13] P. Neddermann, J. Jiricny, Efficient removal of uracil from G:U mispairs by the mismatch-specific thymine DNA glycosylase from HeLa cells, Proc. Natl. Acad. Sci. U.S.A. 91 (1994) 1642–1646.
[14] M. Saparbaev, J. Laval, 3,N^4-ethenocytosine, a highly mutagenic adduct, is a primary substrate for *Escherichia coli* double-stranded uracil-DNA glycosylase and human mismatch-specific thymine DNA glycosylase, Proc. Natl. Acad. Sci. U.S.A. 95 (1998) 8508–8513.
[15] E. Lutsenko, A.S. Bhagwat, The role of the *Escherichia coli* Mug protein in the removal of uracil and 3, N^4-ethenocytosine from DNA, J. Biol. Chem. 274 (1999) 31034–31038.
[16] R.J. Boorstein, A. Cummings Jr., D.R. Marenstein, M.K. Chan, Y. Ma, T.A. Neubert, S.M. Brown, G.W. Teebor, Definitive identification of mammalian 5-hydroxymethyluracil DNA *N*-glycosylase activity as SMUG1, J. Biol. Chem. 276 (2001) 41991–41997.
[17] H.S. Pettersen, O. Sundheim, K.M. Gilljam, G. Slupphaug, H.E. Krokan, B. Kavli, Uracil-DNA glycosylases SMUG1 and UNG2 coordinate the initial steps of base excision repair by distinct mechanisms, Nucleic Acids Res. 35 (2007) 3879–3892.
[18] M. Sandigursky, A. Faje, W.A. Franklin, Characterization of the full length uracil-DNA glycosylase in the extreme thermophile *Thermotoga maritima*, Mutat. Res. 485 (2001) 187–195.
[19] M. Sandigursky, W.A. Franklin, Uracil-DNA glycosylase in the extreme thermophile *Archaeoglobus fulgidus*, J. Biol. Chem. 275 (2000) 19146–19149.
[20] A.A. Sartori, P. Schar, S. Fitz-Gibbon, J.H. Miller, J. Jiricny, Biochemical characterization of uracil processing activities in the hyperthermophilic archaeon *Pyrobaculum aerophilum*, J. Biol. Chem. 276 (2001) 29979–29986.
[21] A.A. Sartori, S. Fitz-Gibbon, H. Yang, J.H. Miller, J. Jiricny, A novel uracil-DNA glycosylase with broad substrate specificity and an unusual active site, EMBO J. 21 (2002) 3182–3191.
[22] V. Starkuviene, H.J. Fritz, A novel type of uracil-DNA glycosylase mediating repair of hydrolytic DNA damage in the extremely thermophilic eubacterium *Thermus thermophiles*, Nucleic Acids Res. 30 (2002) 2097–2102.
[23] J.H. Chung, E.K. Im, H.Y. Park, J.H. Kwon, S. Lee, J. Oh, K.C. Hwang, J.H. Lee, Y. Jang, A novel uracil-DNA glycosylase family related to the helix-hairpin-helix DNA glycosylase superfamily, Nucleic Acids Res. 31 (2003) 2045–2055.
[24] J.A.R.G. Barbosa, J. Sivaraman, Y. Li, R. Larocque, A. Matte, J.D. Schrag, M. Cygler, Mechanism of action and NAD^+-binding mode revealed by the crystal structure of L-histidinol dehydrogenase, Proc. Natl. Acad. Sci. U.S.A. 99 (2002) 1859–1864.
[25] T. Ohta, S. Tokishita, K. Mochizuki, J. Kawase, M. Sakahira, H. Yamagata, UV sensitivity and mutagenesis of the extremely thermophilic eubacterium *Thermus thermophilus* HB27, Genes Environ. 28 (2006) 56–61.
[26] T. Ohta, S. Tokishita, R. Imazuka, I. Mori, J. Okamura, H. Yamagata, β-Glucosidase as a reporter for the gene expression studies in *Thermus thermophilus* and constitutive expression of DNA repair genes, Mutagenesis 21 (2006) 255–260.
[27] J. Hoseki, A. Okamoto, R. Masui, T. Shibata, Y. Inoue, S. Yokoyama, S. Kuramitsu, Crystal structure of a family 4 uracil-DNA glycosylase from *Thermus thermophilus* HB8, J. Mol. Biol. 333 (2003) 515–526.
[28] M. Watanabe-Akanuma, R. Woodgate, T. Ohta, Enhanced generation of A:T → T:A transversions in a *recA730 lexA*(Def) mutant of *Escherichia coli*, Mutation Res. 373 (1997) 61–66.
[29] T. Ohta, M. Watanabe-Akanuma, H. Yamagata, A comparison of mutation spectra detected by the *Escherichia coli* Lac^+ reversion assay and the *Salmonella typhimurium* His^+ reversion assay, Mutagenesis 15 (2000) 317–323.

Mutation Research 673 (2009) 74–77

Contents lists available at ScienceDirect

Mutation Research/Genetic Toxicology and Environmental Mutagenesis

journal homepage: www.elsevier.com/locate/gentox
Community address: www.elsevier.com/locate/mutres

Short communication

Increased formation of gastric N^2-ethylidene-2′-deoxyguanosine DNA adducts in aldehyde dehydrogenase-2 knockout mice treated with ethanol

Haruna Nagayoshi[a,b], Akiko Matsumoto[c], Ryuhei Nishi[b], Toshihiro Kawamoto[d], Masayoshi Ichiba[c], Tomonari Matsuda[b,*]

[a] Osaka Prefectural Institute of Public Health, Osaka 537-0025, Japan
[b] Research Center for Environmental Quality Management, Kyoto University, Otsu 520-0811, Japan
[c] Department of Social and Environmental Medicine, Saga University, Saga 849-8501, Japan
[d] Department of Environmental Health, University of Occupational and Environmental Health, Kitakyusyu, Fukuoka 807-8555, Japan

ARTICLE INFO

Article history:
Received 2 September 2008
Received in revised form 7 October 2008
Accepted 22 November 2008
Available online 3 December 2008

Keywords:
Aldh2 knock-out mouse
Acetaldehyde
Stomach
LC/MS/MS
N^2-Ethylidene-2′-deoxyguanosine
N^2-Ethyl-2′-deoxyguanosine

ABSTRACT

We analyzed an acetaldehyde-derived DNA adduct, N^2-ethylidene-2′-deoxyguanosine (N^2-Eti-dG) in stomach DNA of aldehyde dehydrogenase (*Aldh*)-2-knockout mice that were fed with alcohol to determine effects of alcohol consumption and *Aldh2* genotype on the level of DNA damage in stomach. *Aldh2*-active(+/+), heterozygote(+/−) and knockout(−/−) mice were fed 20% ethanol for 5 weeks, then the level of N^2-Eti-dG in stomach was determined by liquid chromatography tandem mass spectrometry. The average N^2-Eti-dG level in DNA from untreated mice was not significantly different among *Aldh2* genotypes (2.0–3.1 adducts/10^7 bases), however, the average N^2-Eti-dG level in DNA from ethanol-treated mice was 4.8 ± 2.6 adducts/10^7 bases in *Aldh2*+/+ mice, 7.9 ± 1.1 adducts/10^7 bases in *Aldh2*+/− mice, and 48.6 ± 12.0 adducts/10^7 bases in *Aldh2*−/− mice, respectively. Our data clearly showed that alcohol drinking caused DNA damage in stomach, which was *Aldh2* genotype-dependent in this experimental animal model. This result suggests that heavy-alcohol drinking and *Aldh2* deficiency might be risk factors of stomach cancer.

1. Introduction

Alcohol intake is a risk factor for several types of cancer. Many studies of different design and in different populations around the world have consistently shown that daily alcohol consumption is a risk factor for cancers of oral cavity, pharynx, larynx and oesophagus [1–3]. Daily consumption of around 50 g of ethanol increases the risk for these cancers two to three times [1]. Moreover, many epidemiological studies consistently suggested that alcohol consumption is associated with an increased risk of liver cancer, breast cancer and colorectal cancer. In the case of stomach cancer, although many studies failed to show evidence of an association between alcohol drinking and stomach cancer risk, there are several other studies that clearly showed an association [4–7]. Endoscopic screening has yielded a higher rate of detection of gastric carcinoma in alcoholic Japanese men (1.7%) than in the general male Japanese population (0.2%) [8].

When the alcohol is assimilated, ethanol is metabolized and excreted in two steps. Firstly, ethanol is oxidized to acetaldehyde by alcohol dehyderogenase (ADH) and the ADH holoenzyme may exist as either a homodimer or heterodimer of α, β and γ subunits, encoded by *ADH1A*, *ADH1B* and *ADH1C*. The second step is the oxidation of acetaldehyde to acetate by aldehyde dehydrogenase (ALDH) or inducible cytochrome P450 2E1. Among human ALDH isozymes, the Michaelis constant (K_m) value of mitochondrial ALDH2 is predominantly low and that is why ALDH2 is a key enzyme for acetaldehyde metabolism. ALDH2 is a homotetrameric enzyme and the protein encoded by *ALDH2*2* has glutamic acid to lysin substitution at residue 487, resulting in an inactive subunit and dysfunctional ALDH2. ALDH2 has three types of polymorphism: *ALDH2*1/2*1*, an active form; *ALDH2*1/2*2*, a deficient form and *ALDH2*2/2*2* an inactive form. In *ALDH2*1/2*2* or *ALDH2*2/2*2* individuals, aldehyde remains in the body longer than in active *ALDH2*1/2*1* individuals and carcinogenic potential of acetaldehyde is exhibited [2,9].

Several reports described association between *ALDH2* genetic polymorphism and gastric cancers. Yokoyama and his colleagues reported that *ALDH2* genetic polymorphism was closely related with gastric cancer risk in Japanese alcoholic patients [10–12]. Chronic atrophic gastritis (CAG), which in many cases is induced

Abbreviations: ADH, alcohol dehydrogenase; ALDH, aldehyde dehydrogenase; N^2-Eti-dG, N^2-ethylidene-2′-deoxyguanosine; N^2-Et-dG, N^2-ethyl-2′-deoxyguanosine; CAG, chronic atrophic gastritis; α-*S*-Me-γ-OH-PdG, α-*S*-methyl-γ-hydroxy-1, N^2-propano-2′-deoxyguanosine; α-*R*-Me-γ-OH-PdG, α-*R*-methyl-γ-hydroxy-1, N^2-propano-2′-deoxyguanosine; 8-oxo-dG, 8-oxo-7,8-dihydro-2′-deoxyguanosine; LC/MS/MS, liquid chromatography tandem mass spectrometry.

* Corresponding author. Tel.: +81 75 753 5052; fax: +81 75 753 5052.
E-mail address: matsuda@z05.mbox.media.kyoto-u.ac.jp (T. Matsuda).

1383-5718/$ – see front matter © 2008 Elsevier B.V. All rights reserved.
doi:10.1016/j.mrgentox.2008.11.009

by *Helicobacter pylori* infection, and *ALDH2*1/2*2* are independently associated with increase of gastric cancer risk in Japanese alcoholic patients. Combinations of CAG and *ALDH2*1/2*2* showed greater risks of gastric carcinoma (*OR* = 39.2 for severe CAG plus *ALDH2*1/2*2*, CAG negative plus *ALDH2*1/2*1* was used as a reference) [11]. Zhang et al. also reported that another polymorphism of *ALDH2* found in Europeans, *ALDH2* Ex1 + 82A > G, is associated with alcohol-related increase in gastric cancer risk in Poland, although biochemical properties of this new polymorphism are not well understood [13]. These data suggest that acetaldehyde plays crucial roles in the development of stomach cancers.

Acetaldehyde is thought to be a tumor initiator because of its mutagenic and DNA-damaging properties [14–17]. Acetaldehyde forms several DNA adducts such as N^2-ethyl-2′-deoxyguanosine (N^2-Et-dG), α-*S*- and α-*R*-methyl-γ-hydroxy-1, N^2-propano-2′-deoxyguanosine (α-*S*-Me-γ-OH-PdG and α-*R*-Me-γ-OH-PdG) [18–20]. Aside from these stable DNA adducts, reaction of acetaldehyde results in the formation of an unstable and more abundant DNA adduct, N^2-ethylidene-dG (N^2-Eti-dG). Wang et al. showed that N^2-Eti-dG in human liver DNA is relatively stable and that the presence of this adduct could be confirmed by detection of N^2-Et-dG after reduction of DNA during isolation and enzymatic hydrolysis [21]. Because N^2-Eti-dG is the most abundant DNA adduct among acetaldehyde-derived adducts, it would be the sensitive biomarker of acetaldehyde exposure. In this study, we analyzed N^2-Eti-dG in stomach DNA of *Aldh2*-knockout mice that were exposed to alcohol to determine the effects of alcohol consumption and *Aldh2* genotype on the level of DNA damage in the stomach.

2. Materials and methods

2.1. Animal treatment

10–11-week old male *ALDH2*-knockout mice, which had been backcrossed C57BL6, were obtained from the Department of Environmental Health, University of Occupational and Environmental Health, Japan. The mice were used in conformity with the regulation of the committee on animal experiments of Saga University, Japan. The genotype of *ALDH2* was determined by polymerase chain reaction according to the method of Kitagawa et al. using genomic DNA from their ears and lungs [22].

The mice were fed 20% ethanol solution and standard hard feed CR-LPF (348 kcal/100 g) (Charles River Japan, Yokohama, Japan) for 5 weeks. They were then killed and stomach tissue specimens were collected, frozen in liquid nitrogen and stored at −80 °C until they were analyzed.

2.2. DNA isolation from mice stomach

For quantification of 8-oxo-7,8-dihydro-2′-deoxyguanosine (8-oxo-dG), mouse stomach DNA was extracted and purified by using Gentra® puregene™ tissue kit (QIAGEN). The protocol was performed basically as per manufacture's instructions except that desferroxamine (final concentration: 0.1 mM) was added to all solutions to avoid formation of oxidative adducts during the purification step.

For quantification of N^2-Eti-dG, DNA was isolated as described previously [23]. Gentra Puregen tissue kit was used. The procedure was basically as per manufacture's instructions except for adding $NaBH_3CN$ to all solutions (final concentration: 100 mM). After the purification step, DNA was dissolved in 10 mM Tris–HCl/5 mM EDTA buffer (pH 7.0), extracted with chloroform and precipitated with ethanol.

2.3. DNA adduct standards and their stable isotope

8-oxo-dG was purchased from Sigma–Aldrich Japan, Tokyo, Japan. [U-$^{15}N_5$] 8-oxo-dG was kindly supplied by Dr. Shibutani at SUNY Stony Brook, USA. N^2-Et-dG and its [U-$^{15}N_5$]-labeled standard was synthesized as described previously [18].

2.4. DNA digestion

20 μg aliquots of DNA were digested into their constituent 2′-deoxyribonucleoside-3′-monophosphate units by the addition of 15 μl of 17 mM citrate plus 8 mM $CaCl_2$ buffer that contained micrococcal nuclease (22.5 U) and spleen phosphodiesterase (0.075 U) plus internal standards. The solutions were mixed and incubated for 3 h at 37 °C, after which alkaline phosphatase (1 U), 10 μl of 0.5 M Tris–HCl (pH 8.5), 5 μl of 20 mM $ZnSO_4$ and 67 μl of distilled water were added and incubated for a further 3 h at 37 °C. The digested sample was extracted twice with methanol. The methanol fractions were evaporated to dryness, resuspended in 50 μl of distilled water and subjected to liquid chromatography tandem mass spectrometry (LC/MS/MS).

2.5. Instrument

LC/MS/MS analyses were performed using a Shimadzu LC system (Shimadzu, Kyoto, Japan) interfaced with a Quattro Ultima triple stage quadrupole MS (Waters-Micromass, Manchester, UK). The LC column was eluted over a gradient that began at a ratio of 5% methanol to 95% water and was changed to 40% methanol over a period of 30 min, changed to 80% methanol from 30 to 35 min and finally returned to the original starting conditions, 5:95, for the remaining 11 min. The total run time was 46 min. Sample injection volumes of 20 μl each were separated on a Shim-pack XR-ODS column (3.0 mm × 75 mm, 2.2 μm) and eluted at a flow rate of 0.2 ml/min. Mass spectral analyses were carried out in positive ion mode with nitrogen as the nebulizing gas. The ion source temperature was 130 °C, the desolvation gas temperature was 380 °C and the cone voltage was operated at a constant 35 V. Nitrogen gas was also used as the desolvation gas (700 l/h) and cone gas (35 l/h) and argon was used to provide a collision cell pressure of 1.5×10^{-3} mbar. Positive ions were acquired in multiple reaction monitoring (MRM) mode. The MRM transitions monitored were as follows: [$^{15}N_5$]8-oxo-dG, *m/z* 288 → 172; 8-oxo-dG, *m/z* 283 → 167; [$^{15}N_5$] N^2-Et-dG, *m/z* 301 → 185 and N^2-Et-dG, *m/z* 295.5 → 179.9. The amount of each adduct was quantified by the ratio of the peak area of the target adducts to that of its stable isotope. Quanlynx (version 4.0) software (Waters-Micromass) was used to create standard curves and to calculate adduct concentrations. The amount of deoxyguanosine was monitored at 254 nm by a Shimadzu SPD-10A UV-Visible detector that was in place before the tandem MS.

3. Results

The mice were fed with water or 20% ethanol and standard hard feed for 5 weeks. Feed intake slightly dropped in the 20% ethanol group, but there was no significant difference amongst the *Aldh2* genotypes. The average ethanol intake in the case of the 20% ethanol group was not significantly different between *Aldh2* genotypes (~23 g/day/kg body wt). Reduction in body weight was observed predominantly in *Aldh2*−/− mice as described in our previous report [24]. After 5 weeks of feeding with water and 20% ethanol, the mice were killed and their stomach DNA was extracted and purified to detect DNA adduct level.

Firstly, we analyzed the level of acetaldehyde-inducible stable DNA adducts, N^2-Et-dG. However, it was not detected in any stomach DNA samples for both alcohol-treated and non-treated mice for any *Aldh2* genotype. Next, to determine acetaldehyde-derived major DNA adduct, N^2-Eti-dG in DNA, we purified stomach DNA using several reagents containing strong reducing agent, $NaBH_3CN$. During the purification procedure, it was expected that N^2-Eti-dG would be converted to stable N^2-Et-dG (Fig. 1). The average N^2-Eti-dG level in DNA from untreated mice was 3.1 ± 2.3 adducts/10^7 bases in *Aldh2*+/+ mice, 2.0 ± 0.6 in *Aldh2*+/− mice, and 2.2 ± 0.4 in *Aldh2*−/− mice, respectively. On the other hand, in 20% ethanol-treated mice, significant N^2-Eti-dG level increase was observed. The average N^2-Eti-dG level in DNA from 20% ethanol-treated mice was 4.8 ± 2.6 adducts/10^7 bases in *Aldh2*+/+ mice, 7.9 ± 1.1 adducts/10^7 bases in *Aldh2*+/− mice, and 48.6 ± 12.0 adducts/10^7 bases in *Aldh2*−/− mice, respectively (Fig. 2A). This data indicated that *Aldh2* genotype has an effect on gastric N^2-Eti-dG level. On the other hand, DNA adduct induced by oxidative stress, 8-oxo-dG, was detected in all samples, but neither alcohol-dependent nor *Aldh2* genotype-dependent change was observed (Fig. 2B).

4. Discussion

Several epidemiological evidences suggested that alcohol consumption is a risk factor of gastric cancer and genotype of *ALDH2* is considered to play an important role in increasing the risk. One animal carcinogenicity study supported the epidemiological observation. Male and female Sprague–Dawley rats fed on 10% ethanol, started at 39 weeks of age and continued until their spontaneous death, showed significantly increased frequency of forestomach

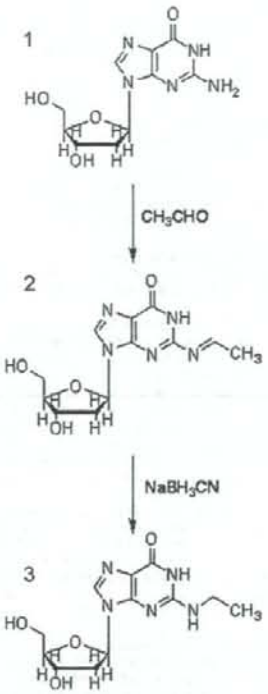

Fig. 1. Formation of acetaldehyde-dG adducts: (1) 2′-deoxyguanosine; (2) N^2-ethylidene-2′-deoxyguanosine (N^2-Eti-dG); (3) N^2-ethyl-2′-deoxyguanosine (N^2-Et-dG) N^2-Eti-dG was easily reduced with $NaBH_3CN$.

acanthoma and carcinoma [25]. However, little other experimental evidence, which support the relationship between *ALDH2* genotype and gastric cancer risk, was available. In this study, we clearly showed that ethanol significantly induced N^2-Eti-dG DNA adducts in mouse stomach, and formation of the DNA adduct was *Aldh2* genotype-dependent. This result is consistent with the report by Ogawa et al. which showed *Aldh2* genotype-dependent incorporation of radioactivity in stomach DNA of mice administered ^3H- or ^{14}C-labeled ethanol [26].

Several pathways are considered for generation of and exposure to acetaldehyde in stomach. A portion of consumed ethanol is absorbed through stomach mucosa. ADH1C is the major ADH expressed in stomach mucosa, and a portion of absorbed ethanol should be metabolized to acetaldehyde on site [9,27]. Ethanol, absorbed from digestive organs, is distributed throughout the body and the majority of it is metabolized in liver where most of the ADHs are expressed (ADH1A, ADH1B, ADH1C, ADH2, ADH3, ADH4 and ADH5) [9], and produced acetaldehyde is distributed throughout the body via circulation, and the stomach may be exposed to acetaldehyde via circulatory fluids. Another important pathway is via saliva. Ethanol contained in saliva is metabolized to acetaldehyde by oral flora [28], and the upper digestive tract, including the stomach, is continuously expose to saliva with high concentration of acetaldehyde.

The concentration of acetaldehyde in saliva after ingesting ethanol is much higher than in blood, and the acetaldehyde concentration in saliva is significantly higher in *ALDH2* deficient individuals than in normal individuals [29,30]. Alcohol challenge test of 0.6 g ethanol/kg body weight of healthy human volunteers resulted in peak acetaldehyde concentration in blood and saliva of 5 and 53 μM, respectively in *ALDH2*1/*1* homozygotes and 25 and 76 μM, respectively in *ALDH2*1/*2* heterozygotes [29]. Taking this into consideration, in this study, the stomach is considered to be exposed to higher concentration of acetaldehyde in *Aldh2*(−/−) mice than *Aldh2*(+/+) mice via both fluid and saliva pathways.

Human stomach mucosa expresses ALDH1, ALDH2 and ALDH3. The most abundant one is ALDH3, however, its K_m value is thought to be several orders of magnitude higher than that of ALDH2 [26,31]. Klyosov et al. reported that the K_m value of human ALDH1, ALDH2 and hamster ALDH3 were 180 μM, 200 nM and 3.6 mM, respectively when acetaldehyde was used as a substrate [32]. Considering realistic blood and salivary acetaldehyde concentration, ALDH3 may not work well in the stomach, and ALDH2 as well as ALDH1 will con-

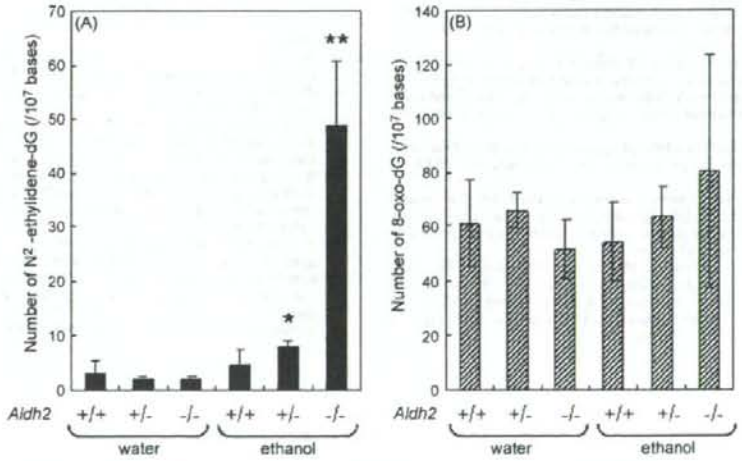

Fig. 2. DNA adduct levels in control and alcohol-treated mice having different *Aldh2* genotypes. Mice were fed with water (*Aldh2*+/+: $n=5$, (+/−): $n=6$, (−/−): $n=5$) or 20% ethanol (*Aldh2*+/+: $n=6$, (+/−): $n=5$, (−/−): $n=4$) for 5 weeks. Stomach DNA samples were purified with $NaBH_3CN$ for the determination of N^2-Eti-dG or without $NaBH_3CN$ for the determination of 8-oxo-dG. Unstable N^2-Eti-dG was reduced to stable N^2-Et-dG under the presence of $NaBH_3CN$. The level of N^2-Eti-dG was detected as N^2-Et-dG by LC/MS/MS. (A) Shows the levels of N^2-Eti-dG in mice stomach DNA and (B) shows the level of 8-oxo-dG in mice stomach. The error bars represent the standard deviation. (*) Significantly increased from water control (+/−); (**) significantly increased from water control (−/−) or ethanol-treated *Aldh2*+/+ mice ($p<0.01$).

tribute to the clearance of acetaldehyde in stomach mucosa. In this situation again, high concentration of acetaldehyde should remain longer in the stomach in *Aldh2*(−/−) mice than in *Aldh2*(+/+) mice.

In conclusion, our data clearly showed that alcohol drinking caused DNA damage in the stomach, and the risk was *ALDH2* genotype-dependent. This strongly supports the epidemiological observations which suggest alcohol drinking and *ALDH2* deficiency are risk factors of stomach cancers.

Conflicts of interest

The authors declare that there are no conflicts of interest.

Acknowledgments

This research was supported in part by Grants-in-aid for Cancer Research from the Ministry of Health, Labor and Welfare of Japan and Grants-in-aid for Scientific Research from the Ministry of Education, Culture, Sports, Science and Technology of Japan. This research was also supported in part by Encouragement of Young Scientists from the Ministry of Education, Culture, Sports, Science and Technology of Japan and by Suntory Limited.

References

[1] R. Baan, K. Straif, Y. Grosse, B. Secretan, F. El Ghissassi, V. Bouvard, A. Altieri, V. Cogliano, Carcinogenicity of alcoholic beverages, Lancet Oncol. 8 (2007) 292–293.
[2] H.K. Seitz, F. Stickel, Molecular mechanisms of alcohol-mediated carcinogenesis, Nat. Rev. Cancer 7 (2007) 599–612.
[3] International Agency for Research on Cancer, IARC monographs on the evaluation of carcinogenic risks to humans Consumption of Alcoholic Beverages and Ethyl Carbamate (Urethane), Summaries and Evaluation, vol. 96, 2007, http://monographs.iarc.fr/ENG/Meetings/96-alcohol.pdf.
[4] T. Shimazu, I. Tsuji, M. Inoue, K. Wakai, C. Nagata, T. Mizoue, K. Tanaka, S. Tsugane, Alcohol drinking and gastric cancer risk: an evaluation based on a systematic review of epidemiologic evidence among the Japanese population, Jpn. J. Clin. Oncol. 38 (2008) 8–25.
[5] T. Ubukata, M. Nakao, A. Ohshima, T. Sobue, H. Tsukuma, K. Morinaga, et al., Drinking and smoking in the etiology of stomach cancer, Nippon Koshu Eisei Zasshi 35 (1988) 286–292 (in Japanese).
[6] I. Kato, S. Tominaga, Y. Ito, S. Kobayashi, Y. Yoshii, A. Matsuura, A. Kameya, T. Kano, A. Ikari, A prospective study of atrophic gastritis and stomach cancer risk, Jpn. J. Cancer Res. 83 (1992) 1137–1142.
[7] S. Kikuchi, T. Nakajima, O. Kobayashi, T. Yamazaki, M. Kikuichi, K. Mori, S. Oura, H. Watanabe, H. Nagawa, R. Otani, N. Okamoto, M. Kurosawa, H. Anzai, T. Konishi, S. Futagawa, N. Mizobuchi, O. Kobori, R. Kaise, Y. Inaba, O. Wada, U-shaped effect of drinking and linear effect of smoking on risk for stomach cancer in Japan, Jpn. J. Cancer Res. 93 (2002) 953–959.
[8] A. Yokoyama, T. Ohmori, T. Muramatsu, S. Higuchi, T. Yokoyama, S. Matsushita, M. Matsumoto, K. Maruyama, M. Hayashida, H. Ishii, Cancer screening of upper aerodigestive tract in Japanese alcoholics with reference to drinking and smoking habits and aldehyde dehydrogenase-2 genotype, Int. J. Cancer 68 (1996) 313–316.
[9] W. Jelski, M. Szmitkowski, Alcohol dehydrogenase (ADH) and aldehyde dehydrogenase (ALDH) in the cancer diseases, Clin. Chim. Acta 395 (2008) 1–5.
[10] A. Yokoyama, T. Muramatsu, T. Omori, T. Yokoyama, S. Matsushita, S. Higuchi, K. Maruyama, H. Ishii, Alcohol and aldehyde dehydrogenase gene polymorphisms and oropharyngolaryngeal, esophageal and stomach cancers in Japanese alcoholics, Carcinogenesis 22 (2001) 433–439.
[11] A. Yokoyama, T. Yokoyama, T. Omori, S. Matsushita, T. Mizukami, H. Takahashi, S. Higuchi, K. Maruyama, H. Ishii, T. Hibi, *Helicobacter pylori*, chronic atrophic gastritis, inactive aldehyde dehydrogenase-2, macrocytosis and multiple upper aerodigestive tract cancers and the risk for gastric cancer in alcoholic Japanese men, J. Gastroenterol. Hepatol. 22 (2007) 210–217.
[12] A. Yokoyama, T. Muramatsu, T. Ohmori, T. Yokoyama, K. Okuyama, H. Takahashi, Y. Hasegawa, S. Higuchi, K. Maruyama, K. Shirakura, H. Ishii, Alcohol-related cancers and aldehyde dehydrogenase-2 in Japanese alcoholics, Carcinogenesis 19 (1998) 1383–1387.
[13] F.F. Zhang, L. Hou, M.B. Terry, J. Lissowska, A. Morabia, J. Chen, M. Yeager, W. Zatonski, S. Chanock, W.H. Chow, Genetic polymorphisms in alcohol metabolism, alcohol intake and the risk of stomach cancer in Warsaw, Poland, Int. J. Cancer 121 (2007) 2060–2064.
[14] P.J. Brooks, J.A. Theruvathu, DNA adducts from acetaldehyde: implications for alcohol-related carcinogenesis, Alcohol 35 (2005) 187–192.
[15] T. Matsuda, M. Kawanishi, T. Yagi, S. Matsui, H. Takebe, Specific tandem GG to TT base substitutions induced by acetaldehyde are due to intra-strand crosslinks between adjacent guanine bases, Nucleic Acids Res. 26 (1998) 1769–1774.
[16] T. Matsuda, I. Terashima, Y. Matsumoto, H. Yabushita, S. Matsui, S. Shibutani, Effective utilization of N^2-ethyl-2′-deoxyguanosine triphosphate during DNA synthesis catalyzed by mammalian replicative DNA polymerases, Biochemistry 38 (1999) 929–935.
[17] I. Terashima, T. Matsuda, T.W. Fang, N. Suzuki, J. Kobayashi, K. Kohda, S. Shibutani, Miscoding potential of the N^2-ethyl-2′-deoxyguanosine DNA adduct by the exonuclease-free Klenow fragment of *Escherichia coli* DNA polymerase I, Biochemistry 40 (2001) 4106–4114.
[18] J.L. Fang, C.E. Vaca, Detection of DNA adducts of acetaldehyde in peripheral white blood cells of alcohol abusers, Carcinogenesis 18 (1997) 627–632.
[19] M. Wang, E.J. Mcintee, G. Cheng, Y. Shi, P.W. Villalta, S.S. Hecht, Identification of DNA adducts of acetaldehyde, Chem. Res. Toxicol. 13 (2000) 1149–1157.
[20] T. Matsuda, H. Yabushita, R.A. Kanaly, S. Shibutani, A. Yokoyama, Increased DNA damage in ALDH2-deficient alcoholics, Chem. Res. Toxicol. 19 (2006) 1374–1378.
[21] M. Wang, N. Yu, L. Chen, P.W. Villalta, J.B. Hochalter, S.S. Hecht, Identification of an acetaldehyde adduct in human liver DNA and quantitation as N^2-ethyldeoxyguanosine, Chem. Res. Toxicol. 19 (2006) 319–324.
[22] K. Kitagawa, T. Kawamoto, N. Kunugita, T. Tsukiyama, K. Okamoto, A. Yoshida, K. Nakayama, Aldehyde dehydrogenase (ALDH) 2 associates with oxidation of methoxyacetaldehyde; in vitro analysis with liver subcellular fraction derived from human and *Aldh2* gene targeting mouse, FEBS Lett. 476 (2000) 306–311.
[23] T. Matsuda, A. Matsumoto, M. Uchida, R.A. Kanaly, K. Misaki, S. Shibutani, T. Kawamoto, K. Kitagawa, K.I. Nakayama, K. Tomokuni, M. Ichiba, Increased formation of hepatic N^2-ethylidene-2′-deoxyguanosine DNA adducts in aldehyde dehydrogenase 2-knockout mice treated with ethanol, Carcinogenesis 28 (2007) 2363–2366.
[24] A. Matsumoto, T. Kawamoto, F. Mutoh, T. Isse, T. Oyama, K. Kitagawa, K.I. Nakayama, M. Ichiba, Effects of 5-week ethanol feeding on the liver of aldehyde dehydrogenase 2 knockout mice, Pharmacogenet. Genomics 18 (2008) 847–852.
[25] M. Soffritti, F. Belpoggi, D. Cevolani, M. Guarino, M. Padovani, C. Maltoni, Results of long-term experimental studies on the carcinogenicity of methyl alcohol and ethyl alcohol in rats, Annu. N. Y. Acad. Sci. 982 (2002) 46–69.
[26] M. Ogawa, T. Oyama, T. Isse, K. Saito, Y. Tomigahara, Y. Endo, T. Kawamoto, A comparison of covalent binding of ethanol metabolites to DNA according to *Aldh2* genotype, Toxicol. Lett. 168 (2007) 148–154.
[27] S.J. Yin, T.C. Cheng, C.P. Chang, Y.J. Chen, Y.C. Chao, H.S. Tang, T.M. Chang, C.W. Wu, Human stomach alcohol and aldehyde dehydrogenases (ALDH): a genetic model proposed for ALDH III isozymes, Biochem Genet 26 (1988) 343–360.
[28] M. Muto, Y. Hitomi, A. Ohtsu, H. Shimada, Y. Kashiwase, H. Sasaki, S. Yoshida, H. Esumi, Acetaldehyde production by non-pathogenic *Neisseria* in human oral microflora: implications for carcinogenesis in upper aerodigestive tract, Int. J. Cancer 88 (2000) 342–350.
[29] S. Vakevainen, J. Tillonen, M. Salaspuro, 4-Methylpyrazole decreases salivary acetaldehyde levels in aldh2-deficient subjects but not in subjects with normal aldh2, Alcohol Clin. Exp. Res. 25 (2001) 829–834.
[30] A. Yokoyama, E. Tsutsumi, H. Imazeki, Y. Suwa, C. Nakamura, T. Mizukami, T. Yokoyama, Salivary acetaldehyde concentration according to alcoholic beverage consumed and aldehyde dehydrogenase-2 genotype, Alcohol Clin. Exp. Res. 32 (2008) 1607–1614.
[31] Y. Alnouti, C.D. Klaassen, Tissue distribution, ontogeny, and regulation of aldehyde dehydrogenase (Aldh) enzymes mRNA by prototypical microsomal enzyme inducers in mice, Toxicol. Sci. 101 (2008) 51–64.
[32] A.A. Klyosov, L.G. Rashkovetsky, M.K. Tahir, W.M. Keung, Possible role of liver cytosolic and mitochondrial aldehyde dehydrogenases in acetaldehyde metabolism, Biochemistry 35 (1996) 4445–4456.

Article

Oxidative DNA Damage in *XPC*-Knockout and Its Wild Mice Treated with Equine Estrogen

Yoshinori Okamoto, Pei-Hsin Chou, Sung Yeon Kim, Naomi Suzuki, Y. R. Santosh Laxmi, Kanako Okamoto, Xiaoping Liu, Tomonari Matsuda, and Shinya Shibutani

Chem. Res. Toxicol., **2008**, 21 (5), 1120-1124• DOI: 10.1021/tx700428m • Publication Date (Web): 01 May 2008

Oxidative DNA Damage in *XPC*-Knockout and Its Wild Mice Treated with Equine Estrogen

Yoshinori Okamoto,[†] Pei-Hsin Chou,[‡] Sung Yeon Kim,[†,§] Naomi Suzuki,[†] Y. R. Santosh Laxmi,[†] Kanako Okamoto,[†] Xiaoping Liu,[†] Tomonari Matsuda,[‡] and Shinya Shibutani*[,†]

Laboratory of Chemical Biology, Department of Pharmacological Sciences, State University of New York at Stony Brook, Stony Brook, New York 11794-8651, and Research Center for Environmental Quality Management, Kyoto University, Otsu, Shiga, 520-0811, Japan

Received December 6, 2007

Long-term hormone replacement therapy with equine estrogens is associated with a higher risk of breast, ovarian, and endometrial cancers. Reactive oxygen species generated through redox cycling of equine estrogen metabolites may damage cellular DNA. Such oxidative stress may be linked to the development of cancers in reproductive organs. Xeroderma pigmentosa complementation group C-knockout (*Xpc*-KO) and wild-type mice were treated with equilenin (EN), and the formation of 7,8-dihydro-8-oxodeoxyguanosine (8-oxodG) was determined as a marker of typical oxidative DNA damage, using liquid chromatography electrospray tandem mass spectrometry. The level of hepatic 8-oxodG in wild-type mice treated with EN (5 or 50 mg/kg/day) was significantly increased by approximately 220% after 1 week, as compared with mice treated with vehicle. In the uterus also, the level of 8-oxodG was significantly increased by more than 150% after 2 weeks. Similar results were observed with *Xpc*-KO mice, indicating that *Xpc* does not significantly contribute to the repair of oxidative damage. Oxidative DNA damage generated by equine estrogens may be involved in equine estrogen carcinogenesis.

Introduction

Hormone replacement therapy (HRT)[1] is widely used by postmenopausal women to alleviate menopausal symptoms and to protect against osteoporosis. In the United States, more than 40% of women in this demographic currently receive HRT, with Premarin (Wyeth-Ayerst) being one of the most commonly used products (*1*). However, HRT is associated with a significantly increased risk of breast, ovarian, and endometrial cancers (*2–4*). Premarin, composed of approximately 30% equilin (EQ), 10% equilenin (EN), and other estrogens, is frequently used for this purpose (*1*). Like human estrogens, EN and EQ are hydroxylated to 4-hydroxyequilenin (4-OHEN) and 4-hydroxyequilin (4-OHEQ), respectively (*1*) (Figure 1). 4-OHEN is rapidly autoxidized to an *o*-quinone, which reacts readily with DNA in vitro, resulting in the formation of bulky DNA adducts (*1, 5, 6*). 4-OHEQ is also autoxidized to an *o*-quinone that isomerizes to 4-OHEN-*o*-quinone; therefore, 4-OHEQ produces DNA adducts identical to those generated by 4-OHEN (*7*). Mutagenic events induced by 4-OHEQ were observed in a *supF* shuttle vector plasmid propagated in human cells (*8*). 4-OHEN-induced DNA adducts were highly miscoded during translesion synthesis catalyzed by human DNA polymerases (*9–11*). Equine estrogen-derived DNA adducts have been detected in the mammary fat pads of rats treated with 4-OHEN (*12*), in breast tumor and adjacent normal tissues of several patients receiving HRT, and in paraffin-embedded breast tumor tissues (*13*).

Redox cycling between the *o*-quinone of 4-OHEN and its semiquinone radical generates reactive oxygen species (ROS) such as superoxide, hydrogen peroxide, and ultimately reactive hydroxyl radicals (*14*) (Figure 1). When 4-OHEN was incubated with DNA or exposed to breast cancer cells in culture, increased formation of 7,8-dihydro-8-oxodeoxyguanosine (8-oxodG) lesions, a typical marker of oxidative DNA damage, was detected (*14–18*). Similar phenomena were observed when 4-OHEN was injected directly into the mammary fat pads of rats (*12*). 8-OxodG is a miscoding and mutagenic lesion (*19–21*). Therefore, oxidative DNA damage induced by equine estrogens may also be involved in carcinogenesis. If equine estrogens produce mutagenic DNA lesions in breast, ovarian, and endometrial tissues of women receiving HRT, such mutagenic DNA adducts may contribute to the initiation of these cancers. The equine estrogen-derived DNA adducts therefore provide biomarkers useful in evaluating the risk of HRT on an individual basis.

Xpc-knockout (*Xpc*-KO) mice are deficient in both alleles of mouse xeroderma pigmentosum complementation group C, one of several factors involved in the recognition of a variety of bulky DNA-distorting lesions in nucleotide excision repair (*22*). Recently, a reduction in the rate of repair of 8-oxodG was observed in human keratinocytes and fibroblasts lacking *Xpc*, indicating that *Xpc* plays an unexpected and multifaceted role in cell protection from oxidative DNA damage (*23*).

To explore the oxidative DNA damage induced by equine estrogens in animals, female mice were treated orally with EN. The levels of 8-oxodG in the liver and uterus were determined

* To whom correspondence should be addressed. Tel: 631-444-7849. Fax: 631-444-3218. E-mail: shinya@pharm.stonybrook.edu.
† SUNY at Stony Brook.
‡ Kyoto University.
§ Present address: Department of Pharmacy, Wonkwang University, Iksan Chonbuk 570-709, South Korea.

[1] Abbreviations: HRT, hormone replacement therapy; EQ, equilin; EN, equilenin; 4-OHEQ, 4-hydroxyequilin; 4-OHEN, 4-hydroxyequilenin; 8-oxodG, 8-oxo-7,8-dihydro-2′-deoxyguanosine; dNTP, 2′-deoxynucleoside triphosphate; ROS, reactive oxygen species; *Xpc*, xeroderma pigmentosa complementation group C; PAGE, polyacrylamide gel electrophoresis; HPLC, high-performance liquid chromatography; LC/MS/MS, liquid chromatography electrospray tandem mass spectrometry.

10.1021/tx700428m CCC: $40.75
Published on Web 05/01/2008

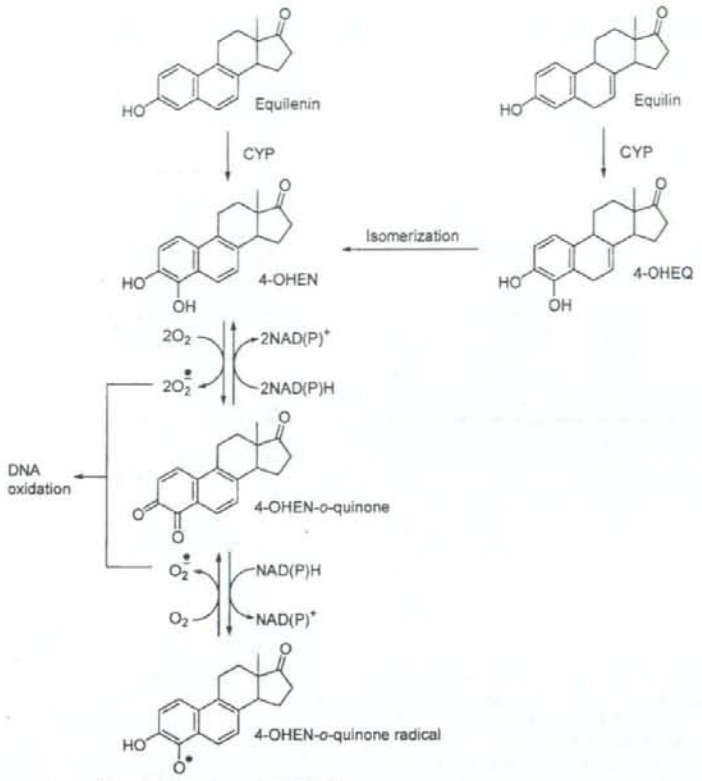

Figure 1. DNA damage and redox cycling mediated through 4-OHEN.

using liquid chromatography electrospray tandem mass spectrometry (LC/MS/MS). Liver was chosen as a major organ metabolizing EN, and uterus was chosen as one of target reproductive organs developing cancer. To evaluate the contribution of *Xpc* in the removal of oxidative DNA damage, EN was also administered to *Xpc*-KO mice. The level of 8-oxodG observed in *Xpc*-KO mice was compared with that observed in wild-type B6129F1 mice.

Materials and Methods

Materials. EN was purchased from Steraloids Inc. (Wilton, NH). 4-OHEN was prepared as described previously (*10*). Desferrioxamine and alkaline phosphatase were obtained from Sigma-Aldrich (St. Louis, MO). $^{15}N_5$-dG was purchased from Cambridge Isotope Laboratory (Andover, MA). Nuclease P1 was obtained from Roche Applied Science (Indianapolis, IN).

Animal Studies. The use of animals was in compliance with the guidelines established by the NIH Office of Laboratory Animal Welfare. *Xpc*-KO mice and mice of the wild-type progenitor strain, B6129F1 (female, 6 weeks old), were purchased from Taconic (Germantown, NY). Animals were acclimated in temperature (22 ± 2 °C) and humidity (55 ± 5%) controlled rooms with a 12 h light−dark cycle for at least 1 week prior to use. Regular laboratory chow and tap water were allowed ad lib. Mice were treated orally (p.o.) with EN (5 or 50 mg/kg/day) for 1 or 2 weeks. Control mice were treated with an identical volume of corn oil. Mice were euthanized by CO_2 asphyxiation at 24 h after the final treatment and then subjected to open thoracotomy. The liver and uterus were removed quickly, frozen, and stored at −80 °C until DNA extraction.

Preparation of DNA Samples. DNA was extracted from the tissue by a modified method of Wang et al. (*24*). To prevent artifactual 8-oxodG formation during DNA extraction, desferrioxamine was used as an antioxidant, as demonstrated in interlaboratory validation study organized by the European Standards Committee on Oxidative DNA Damage (*25*). The tissue (100 mg) was homogenized at 4 °C in 0.2 mL of lysis solution A (320 mM sucrose, 5 mM $MgCl_2$, 10 mM Tris-HCl, 0.1 mM desferrioxamine, pH 7.5, and 1% Triton X-100) using a disposable pellet pestle (Kimble/Kontes, Vineland, NJ). After the tissue was ground, the homogenate was subjected to centrifugation at 10000*g* for 20 s at 4 °C. One milliliter of lysis solution A was added to the pellet and agitated by vortexing. These steps were repeated twice. After centrifugation, 200 μL of solution B (10 mM Tris-HCl, 5 mM EDTA-Na_2, and 0.15 mM desferrioxamine, pH 8.0) and 20 μL of 10% SDS were added to the pellet. The mixture was vortexed for 10 s and incubated at 37 °C for 10 min for suspension of the pellet and to allow for complete lysis of the nuclear membrane. After the addition of 2.7 μg of RNase T_1 and 10 μg of RNase A in a buffer (10 mM Tris-HCl, 1 mM EDTA, and 2.5 mM desferrioxamine, pH 7.4), the samples were incubated at 50 °C for 15 min. Following incubation, 10 μL of Qiagen proteinase K solvent was added, and the samples were incubated for 1 h at 37 °C. After the addition of 0.3 mL of NaI solution (7.6 M NaI, 40 mM Tris-HCl, 20 mM EDTA-Na_2, and 0.3 mM desferrioxamine, pH 8.0), DNA was precipitated by the addition of 500 μL of 2-propanol. The DNA lump was fished out and washed twice with 40% 2-propanol. Finally, the recovered DNA was dried and dissolved in 500 μL of distilled water. The concentration of DNA was determined by UV spectroscopy as 50 μg/mL = $O.D._{260nm}$ 1.0.

Determination of 8-OxodG by LC/MS/MS Analysis. The level of 8-oxodG was determined using LC/MS/MS [high-performance liquid chromatography (HPLC), a Shimadzu LC-10ADvp pump and SIL-10AD autoinjector; MS/MS, Waters-Micromass Quattro Ultima Pt Triple Quadrupole mass spectrometer]. To quantify

8-oxodG accurately, $^{15}N_5$-8-oxodG was prepared from $^{15}N_5$-dG, whose all five Ns in the guanine base were replaced by ^{15}N (Cambridge Isotope Laboratory), following a method developed previously (*26*), and used as an internal standard. The DNA (25 μg) was mixed with $^{15}N_5$-8-oxodG (500 pg) and digested at 37 °C for 3 h with nuclease P1 (4 unit) in 114 μL of buffer mixture [100 μL of 30 mM sodium acetate buffer containing 10 mM 2-mercaptoethanol, pH 5.3; 5 μL of 20 mM $ZnSO_4$; 5 μL of $^{15}N_5$-8-oxodG solution (5 ng/mL); 4 μL of nuclease P1 solution (1 unit/μL); and 3 units of alkaline phosphatase]. After incubation, 20 μL of 0.5 M Tris-HCl, pH 8.5, was added and incubated for 3 h. The enzymes were methanol-precipitated, and the supernatant containing the nucleoside was evaporated and reconstituted with 100 μL of water.

The LC column was eluted over a gradient that began at a ratio of 2% methanol to 98% water and was changed to 40% methanol over a period of 40 min, changed to 80% methanol from 40 to 45 min, and finally returned to the original starting conditions, 2:98, for the remaining 15 min. The total run time was 60 min. Sample injection volumes of 50 μL each were separated on a Shim-pack FC-ODS column (150 mm × 4.6 mm) and eluted at a flow rate of 0.4 mL/min. Mass spectral analyses were carried out in positive ion mode with nitrogen as the nebulizing gas. The ion source temperature was 130 °C, the desolvation gas temperature was 380 °C, and the cone voltage was operated at a constant 40 V. Nitrogen gas was also used as the desolvation gas (700 L/h) and cone gas (35 L/h), and argon was used as the collision gas at a collision cell pressure of 1.5×10^{-3} mBar. Positive ions were acquired in MRM mode. The MRM transitions were monitored as follows: $^{15}N_5$-8-oxodG (*m/z* 288.8 → 172.8) and 8-oxodG (*m/z* 283.8 → 167.8), respectively. The level of 8-oxodG in the DNA samples was determined by comparing with $^{15}N_5$-8-oxodG. The detection limit was approximately 0.1 adducts in 10^6 bases using 25 μg of DNA. The amount of dG in the DNA digest was monitored by a Simadzu SPD-10A UV−visible detector prior to MS/MS analysis. The level of 8-oxodG lesions was estimated by the following equation: the level of 8-oxodG lesion = (amount of 8-oxodG)/[(amount of dG) × 4].

Statistical Analysis. Results were expressed as means ± standard deviations (SDs). A two-sided student's *t* test was used to evaluate the difference. Values of $p \leq 0.05$ were considered statistically significant from the control group.

Results

The level of 8-oxodG lesions in B6129F1 mice treated p.o. with EN was determined using LC/MS/MS analysis and an internal standard, $^{15}N_5$-8-oxodG (Figure 2). The detection limit for 25 μg of DNA sample was approximately 0.1 adduct/10^6 nucleotides. The level of 8-oxodG in the livers of mice treated with 5 mg/kg EN was significantly increased, 220% after 1 week (6.3 adducts/10^6 nucleotides) and 170% after 2 weeks (4.9 adducts/10^6 nucleotides), as compared with that of mice treated with vehicle (2.9 adducts/10^6 nucleotides) (Table 1). With 50 mg/kg EN treatment, a high level of hepatic 8-oxodG (222%) ($p < 0.01$) was also observed after 1 week; however, no significant increase was detected after 2 weeks.

In the uterus, the background level of 8-oxodG was 3.9 times higher than that observed in the liver (Table 1). Although no significant difference was observed after 1 week of treatment with 5 and 50 mg/kg EN, the levels of uterine 8-oxodG were significantly increased after 2 weeks of treatment, to 150 and 162%, respectively, of the background level.

When *Xpc*-KO mice were treated for 1 week with 5 and 50 mg/kg EN, the hepatic 8-oxodG levels increased 155 and 283%, respectively (Table 1); however, no significant increase of 8-oxodG was detected after 2 weeks, as observed with the wild-type mice. The increases of 8-oxodG level in the wild-type and *Xpc*-KO mice treated for 1 week with 50 mg/kg EN were 3.5 ± 1.0 and 8.8 ± 0.4 adducts/10^6 nucleotides, respectively, when their control levels were subtracted. The 8-oxodG increase in *Xpc*-KO mice was 2.5 times higher than that observed in the wild-type mice ($p < 0.01$). The levels of uterine 8-oxodG were significantly increased to 159 (15.7 adducts/10^6 nucleotides) and 193% (19.1 adducts/10^6 nucleotides) after 2 weeks of treatment with 5 and 50 mg/kg EN, as observed with the wild-type mice.

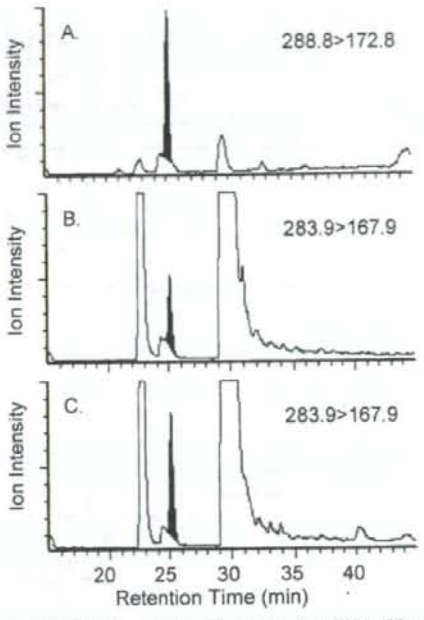

Figure 2. LC/MS/MS analysis of 8-oxodG. The DNA (25 μg) was mixed with $^{15}N_5$-8-oxodG (500 pg) and digested with nuclease P1 and alkaline phosphatase in a buffer. The resulting nucleosides were analyzed using LC/MS/MS, as described in the Materials and Methods. Quantitative analysis of $^{15}N_5$-8-oxodG and 8-oxodG was achieved by monitoring the MS/MS transitions corresponding to the loss of deoxyribose from $^{15}N_5$-8-oxodG (*m/z* 288.8 → 172.8) and 8-oxodG (*m/z* 283.8 → 167.8), respectively. By comparing with internal standard $^{15}N_5$-8-oxodG (A), the level of 8-oxodG in hepatic DNA samples from *Xpc*-KO mouse treated with a vehicle (B) or EN (5 mg/kg/day, p.o. for 2 weeks) (C) was determined.

Table 1. Levels of Hepatic and Uterine 8-OxodG in *Xpc*-KO and Wild-Type Mice Treated Orally with EN

	dose (mg/kg)	duration (weeks)	8-oxodG (adducts/10^6 dNs) wild type	8-oxodG (adducts/10^6 dNs) *Xpc*-KO
			liver	
control			2.9 ± 0.5[a] (100)[b]	4.8 ± 2.4[a] (100)[b]
EN	5.0	1	6.3 ± 1.6* (220)	7.4 ± 3.7 (155)
		2	4.9 ± 2.0* (170)	5.3 ± 0.9 (110)
	50	1	6.4 ± 1.4** (222)	13.6 ± 0.4** (283)
		2	3.4 ± 1.4 (117)	7.7 ± 3.9 (160)
			uterine	
control			11.2 ± 2.2[a] (100)[b]	9.9 ± 4.1[a] (100)[b]
EN	5.0	1	12.9 ± 1.3 (115)	12.1 ± 1.3 (122)
		2	16.8 ± 3.9** (150)	15.7 ± 0.7* (159)
	50	1	11.8 ± 1.1 (105)	10.9 ± 1.6 (110)
		2	18.1 ± 5.4* (162)	19.1 ± 6.4* (193)

[a] Data are expressed as mean values ± SD from three mice in the EN-treated groups and six mice in the control groups. *t* test: *$p < 0.05$ and **$p < 0.01$. [b] The numbers in brackets are % values relative to the control level.